



Lawrence Berkeley Laboratory

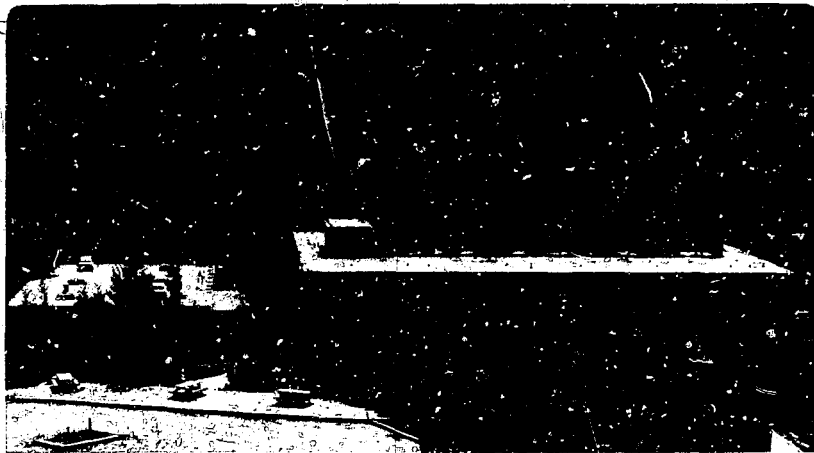
UNIVERSITY OF CALIFORNIA

Materials & Molecular Research Division

MOLECULAR-BEAM SPECTROSCOPY OF INTERHALOGEN MOLECULES

S. A. Sherrow
(Ph.D. Thesis)

August 1983



DISTRIBUTION OF THIS DOCUMENT IS UNLIMITED

LEGAL NOTICE

This book was prepared as an account of work sponsored by an agency of the United States Government. Neither the United States Government nor any agency thereof, nor any of their employees, makes any warranty, express or implied, or assumes any legal liability or responsibility for the accuracy, completeness, or usefulness of any information, apparatus, product, or process disclosed, or represents that its use would not infringe privately owned rights. Reference herein to any specific commercial product, process, or service by trade name, trademark, manufacturer, or otherwise, does not necessarily constitute or imply its endorsement, recommendation, or favoring by the United States Government or any agency thereof. The views and opinions of authors expressed herein do not necessarily state or reflect those of the United States Government or any agency thereof.



Lawrence Berkeley Laboratory

UNIVERSITY OF CALIFORNIA

Materials & Molecular Research Division

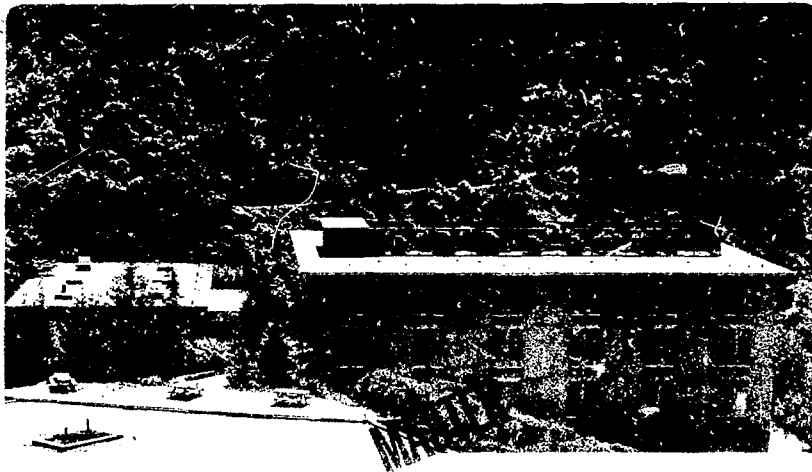
LBL--16545

DE84 001286

MOLECULAR-BEAM SPECTROSCOPY OF INTERHALOGEN MOLECULES

S.A. Sherrow
(Ph.D. Thesis)

August 1983



DISTRIBUTION OF THIS DOCUMENT IS UNLIMITED

Molecular-Beam Spectroscopy
of Interhalogen Molecules

Susan Ann Sherrow

Materials and Molecular Research Division
Lawrence Berkeley Laboratory

and

Department of Chemistry
University of California
Berkeley, CA 94720

ABSTRACT

A molecular - beam electric - resonance spectrometer employing a supersonic nozzle source has been used to obtain hyperfine spectra of $^{79}\text{Br}^{35}\text{Cl}$. Analyses of these spectra and of microwave spectra published by other authors have yielded new values for the electric dipole moment and for the nuclear quadrupole coupling constants in this molecule. The new constants are significantly different from the currently accepted values.

Van der Waals clusters containing chlorine monofluoride have been studied under various expansion conditions by the molecular beam electric deflection method. The structural possibilities indicated by the results are discussed, and cluster geometries are proposed.

ACKNOWLEDGEMENTS

For the assistance, feedback, bad jokes, and morale boosts I enjoyed during my first four years at Berkeley, I thank all the other members of the Winn group. Total control of the radio and thermostat and the undisturbed tranquility of a private office were poor substitutes for their company and encouragement, which I sorely missed during my fifth year.

For welcoming me as a partner in his research project and for trying to teach me everything he knows, I am extremely grateful to Henry Luftman. Many of the sordid details of the work we did together are chronicled in Henry's thesis, which has been an invaluable reference.

I thank Rich Saykally for generously allowing me to use his computer account, and for all of his suggestions and advice.

Thanks to John Muentner, Shelley Shostak, and Steve Harris for providing me with listings of their computer programs.

Thanks to Gloria Pelatowski for expertly drawing four of the figures in chapters II and III.

Most of all, I am indebted to John Winn, who has been my research director, teacher, coworker, and friend. He countered my depression with hope and with humor, my apathy with enthusiasm, and my enthusiasm with still more

enthusiasm. As I have matured as a scientist and (I hope) as a person, I have gained more and more respect for his insights and abilities and appreciation for his efforts. Thanks for everything, John.

This work was supported by the Director, Office of Energy Research, Office of Basic Energy Sciences, Chemical Sciences Division of the U. S. Department of Energy under Contract No. DE-AC03-76SF00098.

TABLE OF CONTENTS

<u>Chapter</u>		<u>Page</u>
I	Molecular Beam Electric Deflection and Resonance	1
	References	7
II	Electric Resonance Spectroscopy of BrCl .	10
	Introduction	10
	Theory	11
	Experiments	15
	Data and Analysis	16
	Conclusions	22
	References	24
III	"Van der Waals" Molecules and Deflection Experiments	26
	Introduction	26
	Experiments	28
	Analysis: ClF Clusters	34
	Analysis: Ar ₂ ClF and Ar ₃ ClF	56
	Conclusions	57
	References	58
Appendix I		60
	References	63
Appendix II		64
	References	89

Chapter I.

Molecular Beam Electric Deflection and Resonance

The experiments discussed in this work were performed on a conventional molecular beam electric resonance spectrometer. The design, construction, and operating characteristics of our particular instrument have been detailed by Luftman,¹ and will not be repeated here. Some additions to Luftman's work are given in the first appendix.

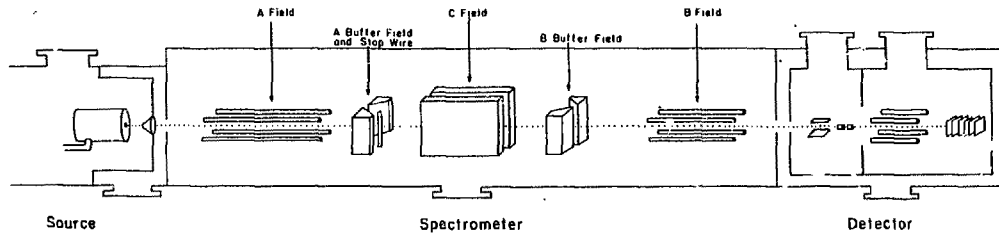
The basic apparatus, shown schematically in Figure I-1, consists of a series of differentially pumped chambers housing a supersonic nozzle beam source; a beam spectrometer which contains a quadrupole state selector, a resonance region, and a quadrupole state analyzer; and a detector which consists of an electron bombardment ionizer, a quadrupole mass filter, and a charged particle multiplier.

Supersonic expansion of the gas mixture yields an intense beam which is translationally,²⁻⁴ rotationally,⁴⁻¹⁰ and, to a lesser extent, vibrationally⁹⁻¹² cold. The exact degree of cooling is a complicated function of the initial source conditions and of the gas mixture. The cooling provided by the expansion enhances the formation of molecular clusters,^{13,14} and the collisionless conditions that prevail after the expansion insure that these species survive the experiment in detectable numbers.

Molecules entering and exiting the spectroscopy chamber pass through the quadrupolar A and B fields. The focussing

Figure I-1

Schematic drawing of the molecular beam electric resonance spectrometer. The beam travels from left to right.



LBL 829-11395

and state selecting properties of these fields toward molecules with permanent dipole moments have been discussed in detail.¹⁵⁻¹⁹ Molecular beam electric deflection experiments which utilize those properties have yielded qualitative information about molecular polarities,^{20,21} dipole moments,²²⁻²⁴ geometries,²⁵ electronic state symmetries,¹⁶ and rotational temperatures.^{4,7} Deflection experiments generally involve blocking the straight-line path from source to detector with some suitable obstacle, and turning up the voltage to the field(s) so that molecules having positive Stark energies are "refocused" around the obstacle and into the detector. The transmission is reported as the ratio of intensities of refocused to straight-through beam. As Maier⁴ and Wicke²⁶ have emphasized, and as Toennies⁷ has clearly shown, the molecules transmitted at a given voltage represent a specific rotational, spatial, and velocity segment of the beam.

The selectivity of the focussing fields provides the basis for molecular beam electric resonance spectroscopy. Typically, the A and B fields are set to transmit a particular rotational state. The selected molecules are oriented by a uniform static field in the resonance region, where they are also subjected to radiofrequency or microwave radiation. The intensity of the transmitted beam is then monitored as a function of the applied frequency, since molecules which have undergone transitions in the resonance region will no longer be focussed into the detector by the B

field. The resulting spectra are characterized by linewidths of a few kilohertz and are analyzed by the usual high resolution microwave methods.

It should be emphasized that in both deflection and resonance experiments the quantity being measured is the number density at the detector of the species of interest itself. Thus, molecules which comprise only a tiny fraction of the total beam may be studied without interference from other species. (Should there be some other species which refocusses similarly to the species of interest and which fragments in the ionizer to give ions of the same mass to charge ratio, velocity selection could be used to distinguish between ions of the same mass to charge ratio which have different molecular origins; generally, however, the spectra obtained are unambiguous.) While the perturbations (static electric fields, radiofrequency and microwave radiation) applied to molecules in the spectroscopy chamber are generally nondestructive, they need not be. Any perturbation which alters the number of molecules reaching the mass spectrometer can be detected without interference. These features have been used to great advantage in the study of molecular clusters and reactive intermediates.

A number of excellent reviews on electric resonance spectroscopy are available.²⁷⁻²⁹ Bowen³⁰ and Luftman¹ provide many obscure (but practical) experimental details and "how to's" which should be read by any persons who intend to attempt experiments of this sort. Luftman

includes detailed theoretical treatments and computer simulations of refocussing and resonance experiments.

The results of electric resonance studies of bromine monochloride (BrCl), and electric deflection experiments involving chlorine monofluoride (ClF) clusters will be presented and discussed in the following chapters.

References for Chapter I

1. H. S. Luftman, Ph.D. Thesis, University of California at Berkeley, 1982.
2. J. B. Anderson and J. B. Fenn, *Phys. Fluids*. 8, 780 (1965); J. B. Anderson, R. P. Andres and J. B. Fenn, in Molecular Beams, edited by J. Ross (John Wiley, New York, 1966); J. B. Anderson, in Molecular Beams and Low Density Gas Dynamics, edited by P. P. Wegener (Dekker, New York, 1974).
3. R. Campargue and A. Lebehot, in Proceedings of the Ninth International Symposium on Rarefied Gas Dynamics, edited by M. Becker and M. Fiebig (Goettingen, 1974).
4. M. Maier, H. S. Luftman and J. S. Winn, submitted to *J. Phys. Chem.*, March 1983.
5. A. Kantrowitz and J. Grey, *Rev. Sci. Inst.* 22, 328 (1951).
6. R. G. Gallagher and J. B. Fenn, *J. Chem. Phys.* 60, 3492 (1974); and *J. Chem. Phys.* 60, 3787 (1974).
7. H. Malthan and J. P. Toennies, in Proceedings of the Ninth International Symposium on Rarefied Gas Dynamics, edited by M. Becker and M. Fiebig (Goettingen, 1974); U. Borkenhagen, H. Malthan and J. P. Toennies, *J. Chem. Phys.* 63, 3173 (1975).
8. S. G. Kukolich, D. E. Oates and J. H. S. Wang, *J. Chem. Phys.* 61, 4686 (1974).
9. K. Bergmann, U. Hefter and P. Hering, *J. Chem. Phys.* 65, 488 (1976).
10. G. M. McClelland, K. L. Saenger, J. J. Valentini, D. R. Herschbach, *J. Phys. Chem.* 83, 947 (1979).
11. R. P. Mariella, S. K. Neoh, D. R. Herschbach, W. Klemperer, *J. Chem. Phys.* 67, 2981 (1977).
12. H. G. Bennewitz and G. Buess, *Chem. Phys.* 28 175 (1978).
13. T. R. Dyke, G. R. Thomasevich, W. Klemperer and W. E. Falconer, *J. Chem. Phys.* 57, 2277 (1972); T. R. Dyke, B. J. Howard and W. Klemperer, *J. Chem. Phys.* 56, 2442 (1972).

14. A. van Deursen and J. Reuss, *Int. J. Masa. Spec. Ion Phys.* **11**, 483 (1973).
15. H. G. Bennowitz, W. Paul. and Ch. Schlier, *Z. Physik* **141**, 6 (1955).
16. R. A. Berg, L. Wharton, W. Klemperer, A. Buchler, J. L. Stauffer, *J. Chem. Phys.* **43**, 2416 (1965).
17. P. R. Brooks, E. M. Jones and K. Smith, *J. Chem. Phys.* **51**, 3073 (1969); E. M. Jones and P. R. Brooks, *J. Chem. Phys.* **53**, 55 (1970).
18. T. C. English and T. F. Gallager, *Rev. Sci. Inst.* **40**, 1484 (1969).
19. J. E. Mosch, S. A. Safron and J. P. Toennies, *Chem. Phys.* **8**, 304 (1975).
20. W. E. Falconer, A. Buchler, J. L. Stauffer, and W. Klemperer, *J. Chem. Phys.* **48**, 312 (1968); J. M. Lisy and W. Klemperer, *J. Chem. Phys.* **72**, 3880 (1980).
21. J. A. Odutola, T. R. Dyke, B. J. Howard, J. S. Muentner, *J. Chem. Phys.* **70**, 4884 (1979).
22. P. J. Dagdigian, J. Graff and L. Wharton, *J. Chem. Phys.* **55**, 4980 (1971); P. J. Dagdigian and L. Wharton, *J. Chem. Phys.* **57**, 1487 (1972).
23. T. L. Story and A. J. Hebert, Lawrence Berkeley Laboratory Report 4310 (1975).
24. J. M. Lisy and W. Klemperer, *J. Chem. Phys.* **70**, 4967 (1979).
25. A. Buchler, J. L. Stauffer, W. Klemperer, L. Wharton, *J. Chem. Phys.* **39**, 2299 (1963); A. Buchler, J. L. Stauffer and W. Klemperer, *J. Chem. Phys.* **40**, 3471 (1964); *J. Am. Chem. Soc.* **86**, 4544 (1964); E. W. Kaiser, J. S. Muentner, W. Klemperer, W. E. Falconer, *J. Chem. Phys.* **53**, 53 (1970).
26. B. Wicke, *J. Chem. Phys.* **63**, 1035 (1975).
27. V. Hughes and L. Grabner, *Phys. Rev.* **79**, 829 (1950).
28. N. F. Ramsey, Molecular Beams (Oxford University Press, London, 1956), Chapter 10.

29. J. C. Zorn and T. C. English, in Advances in Atomic and Molecular Physics, Volume 9, edited by D. R. Bates and I. Estermann (Academic Press, New York, 1973).
30. K. Bowen, Ph.D. Thesis, Harvard University (1978).

Chapter II.

Electric Resonance Spectroscopy of BrCl

Introduction

Halogen and interhalogen molecules have been studied extensively because of their importance in photochemical reactions and their applications in chemical lasers. Microwave and electric resonance spectra have yielded precise values of the molecular constants for the diatomic fluorides¹⁻⁴ and for ICl.⁵ IBr⁶ and BrCl, however, have proven much less tractable because of the complicated nuclear quadrupole interactions and the presence of several isotopic species with similar moments of inertia. Molecular beam electric resonance has the high resolution needed to measure the quadrupole splittings precisely, while monitoring the intensity of a single species. Our first efforts to determine precise molecular hyperfine constants for $^{79}\text{Br}^{35}\text{Cl}$ are reported in this chapter.

The formation of BrCl in mixtures of Br_2 and Cl_2 was first suggested by Balard,⁷ and was confirmed a century later by Gray and Style.⁸ King, Dixon, and Herschbach⁹ proposed, after a crossed beam study, that the actual reaction involves the van der Waals molecule chlorine dimer, $(\text{Cl}_2)_2$, and diatomic bromine. Electronically excited BrCl is formed from the reaction between Br_2 and ClO_2 , which has been studied by Coxon¹⁰ and by Clyne and coworkers.¹¹ The most recent study of BrCl was reported by Farthing and

coworkers,¹² who used laser induced fluorescence to measure the rotational and vibrational relaxation of BrCl in a supersonic beam.

The first microwave spectra of BrCl were reported by Smith, Tidwell, and Williams,¹³ who measured $J=0 \rightarrow 1$ transitions for each of the four molecular isotopes and calculated rotational and nuclear quadrupole coupling constants for each. They also reported an estimated electric dipole moment of 0.57 Debye. In a much later publication, Nair, Hoeft, and Tiemann¹⁴ reported a dipole moment of 0.519 Debye from Stark modulated microwave absorption measurements involving the two most abundant isotopes. The precise hyperfine constants used to calculate this dipole moment were to be revealed in a later publication but, at the time of this work, they have not been reported. The most recent microwave work is that of Willis and Clark,¹⁵ in which the Dunham coefficients and equilibrium constants of ClF, BrF, BrCl, ICl, and IBr were determined from spectra in the millimeter wave region.

Theory

The energy levels of a rotating diatomic molecule with two quadrupolar nuclei in an electric field are solutions of the Hamiltonian:

$$H = H(J,v) + H_{Q1} + H_{Q2} + H_{sr} + H_s.$$

The first term is the usual vibration-rotation Hamiltonian which has as its solution the Dunham¹⁶ expansion:

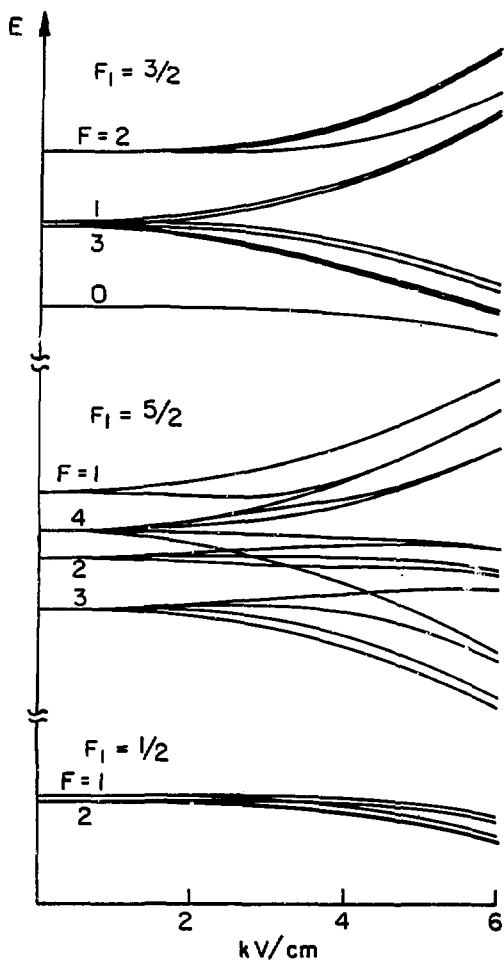
$$E(J, v) = \sum (v + 1/2)^k (J(J+1))^m Y_{k,m},$$

where the $Y_{k,m}$ are the Dunham coefficients, and the summation is over all k and m . H_{Q1} and H_{Q2} are the nuclear quadrupole coupling terms for the two nuclei. The quadrupole matrix elements are nonzero for $J'=J$, $J \pm 2$, and they have been tabulated for two spin 3/2 nuclei by Flygare and Gwinn.¹⁷ H_{sr} contains the spin-rotation interactions and the smaller spin-spin interactions. H_s contains the Stark interaction, which is off-diagonal in J and F by ± 1 and has matrix elements given by Curl and Kinsey.¹⁸ During the analysis of our data we have used computer programs which diagonalize the Hamiltonian and fit molecular parameters to observed transitions. Those programs are discussed in the second appendix.

Figure II-1 shows splitting of the BrCl $J=1$ rotational manifold due to quadrupolar interactions and the Stark effect. The bromine nuclear spin couples to the molecule's rotational angular momentum, yielding three distinct states which are conveniently labelled by the F_1 notation of Bardeen and Townes.¹⁹ The chlorine nuclear spin couples to F_1 , splitting the F_1 levels into sublevels designated by total angular momentum quantum number F . In the presence of an electric field, the F sublevels are split into $2F+1$ Stark levels which are labelled by quantum number M_F . M_F is the projection of the angular momentum along the direction defined by the electric field. The $J=1$ manifold contains 29 distinct energy levels; 19 of these are doubly degenerate.

Figure II-1

Energy levels as a function of electric field strength for the $J=1$ rotational manifold of BrCl.



XBL 836-6223

Experiments

BrCl was prepared by allowing approximately $\frac{1}{2}$ mole of Br₂ (Mallinckrodt Analytical Reagent) and $\frac{1}{2}$ mole of Cl₂ (Matheson research grade) to equilibrate for several hours in a 6 liter monel sample cylinder. The resulting mixture was pressurized to 5300 torr with argon and allowed to equilibrate for an additional 36 hours. Our gas handling system was extremely sensitive to bromine. Because liquid nitrogen trapping did not protect the mechanical pump sufficiently, frequent oil changes and complete pump overhauls were required.

The molecular beam source temperature was 293 K during all experiments, and the source pressure varied from 700-760 torr. Nozzle, stopwire, and detector aperture diameters were 0.010 cm, 0.090 cm, and 0.38 cm, respectively. Major peaks in the mass spectra were identified as Cl, Cl₂, Br, and BrCl. All isotopes were observed in their natural ratios, and the peaks were well resolved. The mass spectra were not extended to the regions of BrCl-containing polymers. The greatest refocussed intensity of ⁷⁹Br³⁵Cl was 35-40 percent of the undeflected beam's intensity, and was fairly constant at A and B field voltages above 20 kV. All spectra were obtained by monitoring the intensity of this parent ion. The mass spectrometer was retuned before each set of experiments.

The rotational and hyperfine constants given by Smith, and the dipole moment of Tiemann were used to calculate

energy levels and hyperfine transitions within the $J=1$ rotational manifold at static electric field strengths of 1054 V/cm and 1515 V/cm. The regions indicated by these calculations were searched for transitions at several radiofrequency amplitudes and focussing field voltages.

Experiments at the lower static field voltage were performed over several consecutive days, with occasional interruptions for the preparation of new sample mixtures. An electrical power surge and failure damaged the spectroscopy chamber components, and the instrument was disassembled and repaired before experiments were resumed at the higher static field voltage. Other experimental procedures were similar to those described by Luftman.²⁰

Data and Analysis

The selection rules applicable to our experiments are:

$$\Delta M_F = 0, \pm 1 \quad \Delta J = 0 \quad \Delta F_1 = 0.$$

The first is an ordinary microwave selection rule for radiation applied parallel and perpendicular to the electric field; the others are consequences of our radiofrequency synthesizer's upper limit of 80 MHz. The additional observability criterion for molecular beam electric resonance transitions is that the initial and final states must have different trajectories in the focussing field.

In our searches for hyperfine transitions we observed very few strong transitions, and these did not fit the pattern predicted by our calculations. We observed several

very weak, but reproducible features. By varying the focussing field voltages and the radiofrequency power we were able to improve their intensity somewhat, but the signal to noise remained quite poor. Our failure to observe the high frequency $F_1 = 3/2$, $F = 2 \rightarrow 3$ and $F_1 = 5/2$, $F = 3 \rightarrow 1$ transitions was most disturbing, since these transitions are isolated, thus easy to assign, and are strongly dependent on the static field strength.

After the experimental work was completed, we developed a line fitting program which enabled us to refit the microwave data for $^{79}\text{Br}^{35}\text{Cl}$ reported by Smith and Tiemann. The results of several fits are collected in Table II-1. The first set of constants results from fitting both quadrupole coupling constants, eqQ , and the ground vibrational state rotational constant, B_0 , to the observed transitions. In the simultaneous fit of the two data sets, three of the transitions recorded by Smith have been omitted in favor of the more precise measurements of Tiemann. The second set of constants results from fitting only the quadrupole coupling constants. The rotational constant and centrifugal distortion constant, D , were calculated from the Dunham coefficients reported by Willis. The constants originally determined by Smith are presented for comparison.

The inherent danger in the procedure of fitting several spectroscopic constants to a few observed transitions is well illustrated. Although the parameter values obtained from such calculations form a self-consistent set, the

Table II-1

Spectroscopic Constants (kHz) Derived from Microwave Data

<u>B₀</u>	<u>eqQ_R</u>	<u>eqQ_{C1}</u>	<u>Source</u>
4559310 ± 60	876800 ± 900	-103600 ± 150	a
4559320 ± 50	876090 ± 710	-100550 ± 1230	b
4559391 ± 4	875127 ± 70	-102469 ± 76	c
4559360 ± 15	875450 ± 200	-102310 ± 280	d
B ₀ =4559381.8 ± 3.2, D=2.1805 ± .0007			e
	875643 ± 270	-101880 ± 460	f
	875008 ± 131	-102269 ± 110	g
	875430 ± 210	-102380 ± 280	h

a Reported in Reference 13.

b 3 parameter fit of data from 13.

c 3 parameter fit of data from 14.

d Simultaneous 3 parameter fit of data from 13, 14.

e Calculated from Dunham coefficients, Reference 15.

f 2 parameter fit of data from 13.

g 2 parameter fit of data from 14.

h Simultaneous 2 parameter fit of data from 13, 14.

Uncertainties reported are one standard deviation.

parameters themselves are so highly correlated that the values determined may be considerably less accurate than the standard deviation of the fitting indicates. Not only do the two data sets yield different values of the hyperfine constants, those values are very different from those of the original Smith publication and the much later review work of Lovas and Tiemann.²¹ We attempted, unsuccessfully, to reproduce the calculations of Smith et al., using the method of Bardeen and Townes¹⁹ which they referenced. In their calculations, it seems, they underestimated the quadrupolar energies and compensated by overestimating the coupling constants. The second fit of the Tiemann data represents, we believe, the most reliable estimates of the coupling constants. The value of eqQ_{C1} is 1340 kHz (nine standard deviations) smaller than the value reported by Smith. This error had unfortunate consequences for our experiments.

Several of the resonances which we observed could not be assigned to $J=1$, but were consistent with our calculations for $J=3$.²² In our analysis, we have included only those transitions assigned to $J=1$. Because our observed resonances all have $\Delta F_1=0$, they are essentially independent of the bromine nuclear quadrupole coupling; they are very sensitive to the chlorine nuclear quadrupole coupling and to the molecular dipole moment. We have fitted the chlorine quadrupole coupling constant, eqQ_{C1} , and the dipole moment, μ , to our data. The results are tabulated in Table II-2. The deviations between calculated and observed resonance

Table II-2

BrCl Spectroscopic Constants Derived from Molecular Beam
Electric Resonance Spectra

Parameter values determined:

$$\text{eqQ}_{Cl} = 102294.6 \pm 9.9 \text{ kHz} \quad \mu = 0.5237 \pm 0.0004 \text{ D}$$

Frequencies (kHz) and Assignments:

<u>F_l</u>	<u>F,M</u>	<u>F',M'</u>	<u>Observed</u>	<u>Calculated</u>	<u>Obs.-Calc.</u>
					1501.6816 V/cm
5/2	1,1	3,1	24923.0	24301.4	-8.4
5/2	3,3	4,3	17562.0	17567.0	-5.9
3/2	3,0	2,1	17502.0	17502.0	0.0
5/2	3,2	4,3	16832.0	16834.9	-2.9
3/2	0,0	3,1	15954.0	15948.6	5.4
3/2	0,0	3,0	15779.0	15784.0	-5.0
3/2	1,1	2,2	15682.0	15692.7	-10.7
3/2	1,0	3,0	3210.0	3206.0	3.9
1/2	2,0	1,1	1624.0	1627.4	-3.4
1/2	1,1	2,1	1550.0	1555.0	-5.0
3/2	1,0	1,1	1220.0	1226.1	-6.1
5/2	2,1	2,2	1044.0	1044.5	-0.5
					1043.6249 V/cm
3/2	0,0	1,1	17816.3	17805.7	10.6
5/2	4,2	3,3	17747.9	17742.4	5.5
5/2	4,1	3,2	17652.9	17643.7	9.2
3/2	2,1	3,1	16674.8	16680.1	-5.3
5/2	3,3	4,4	16662.8	16656.5	6.3
3/2	2,0	3,1	16634.1	16632.3	1.8
5/2	4,3	4,4	636.0	637.3	-1.3
3/2	3,2	3,3	588.0	588.2	-0.2

Correlation Matrix:

<u>eqQ_{Cl}</u>	<u>μ</u>
1.000	
0.045	1.000

Parameter values (kHz) used in calculations:

$$\begin{aligned} B_0 &= 4559381.82 \\ D &= 2.15805 \\ \text{eqQ}_{Br} &= 875007.56 \end{aligned}$$

Uncertainties reported are one standard deviation.

frequencies are consistent with spin-rotation constants of 10 kHz or less, which is in agreement with our estimates according to the procedure given in Townes.²³ The quantity and quality of the data do not justify the inclusion of spin-rotation and spin-spin terms in the fitting.

The chlorine quadrupole coupling constant we have obtained is in good agreement with the microwave results. This is hardly remarkable, since we used calculations which employed those results as aids in assigning the resonances. The value we obtain for the dipole moment is slightly higher than that calculated by Tiemann et al. In Tiemann's analysis of IBr,^{6c} the rotational constant and the quadrupole coupling constants were fitted to a small set of transitions observed at zero electric field. We suspect that is exactly what was done with BrCl, since Willis' Dunham coefficients were not yet available. Because their methods of calculation are quite similar to ours, their unpublished hyperfine parameters should resemble those we obtained from the first fit of their data. As mentioned earlier, we consider the results of the second fit of their data to be the more reliable. Because the chlorine quadrupole coupling and the Stark effect shift the hyperfine levels in the same direction, their slight overestimate of the chlorine coupling constant would lead to a slight underestimate of the electric dipole moment. This explanation becomes more plausible when one considers that they were not able to resolve the Stark splittings. Their

calculation of the dipole moment was based on the intensity weighted average Stark shifts of nine transitions (four of these were $^{81}\text{Br}^{35}\text{Cl}$). Furthermore, it is not clear how much of the line broadening they observed was due to the (admitted) inhomogeneity of their electric field and how much was due to the unresolved Stark splittings.

Conclusions

Because there are so many energy levels and allowed transitions, the fraction of molecules participating in any single transition is small. Although molecular beam electric resonance is an extremely sensitive spectroscopic technique, our particular instrument was characterized by rather poor sensitivity at the time of these experiments. A further complication, which Luftman has discussed, is the drastic dependence of resonance lineshapes and intensities on the radiofrequency power and on the focussing field voltages. Under these circumstances, the location and assignment of transitions become extremely difficult tasks.

The author's own inexperience and the unusual time constraints imposed compounded the difficulties inherent in the experimental work. An important set of transitions was not observed because our searches were within the frequency regions indicated by calculations that employed Smith's original hyperfine parameters. Although a reasonable fit of the molecular constants was obtained, reasonable fits do not, in themselves, guarantee accurate results. Because of

the poor quality of the data, we feel that the assignments reported here are rather tenuous, and that this investigation must be regarded as preliminary. We have, we believe, clearly demonstrated that the currently accepted values of the $^{79}\text{Br}^{35}\text{Cl}$ hyperfine constants are in error, and that more precise experimental work is required if they are to be determined accurately.

Specifically, we recommend that the transitions $F_1=3/2$, $F=2 \rightarrow F_1=1/2$, $F=1$ and $F_1=3/2$, $F=2 \rightarrow F_1=5/2$, $F=3$ be located. These transitions are strongly allowed by microwave and electric resonance selection rules, and are in regions of the spectrum which do not contain hyperfine transitions from other J manifolds.

References for Chapter II

1. ClF: D. A. Gilbert, A. Roberts and P. A. Griswold, Phys. Rev. **76**, 196A (1949); R. E. Davis and J. S. Muentner, J. Chem. Phys. **57**, 2836 (1972); B. Fabricant and J. S. Muentner, J. Chem. Phys. **66**, 5274 (1977).
2. BrF: D. F. Smith, M. Tidwell and D. V. P. Williams, Phys. Rev. **77**, 420L (1950).
3. IF: J. C. McGurk and W. H. Flygare, J. Chem. Phys. **59**, 5742 (1973); E. Tiemann, J. Hoeft and T. Torring, Z. Naturforsch. **28a**, 1405 (1973).
4. J. J. Ewing, H. L. Tigelaar and W. H. Flygare, J. Chem. Phys. **56**, 1957 (1972).
5. ICl: R. T. Weidner, Phys. Rev. **73**, 254 (1948); C. H. Townes, F. R. Merritt and B. D. Wright, Phys. Rev. **73**, 1334, (1948); E. Herbst and W. Steinmetz, J. Chem. Phys. **56**, 5342 (1972).
6. IBr: (a) T. S. Jaseja, J. Mol. Spectrosc. **5**, 445, (1960); (b) E. Tiemann and Th. Moller, Z. Naturforsch. **30a**, 986 (1975); (c) E. Tiemann and A. Dreyer, Chem. Phys. **23**, 231 (1977).
7. Balard, Ann. chim. phys. **32**, 337 (1826).
8. Gray and Style, Proc. Roy. Soc. **A126**, 603 (1934).
9. D. L. King, D. A. Dixon and D. R. Herschbach, J. Am. Chem. Soc. **96**, 3328 (1974).
10. J. A. Coxon, J. Mol. Spectrosc. **50**, 142 (1974).
11. M. A. A. Clyne and S. Toby, J. Photochem. **11**, 87 (1979), and references therein.
12. J. W. Farthing, I. W. Fletcher and J. C. Whitehead, Mol. Phys. **48**, 1067 (1983).
13. D. F. Smith, M. Tidwell and D. V. P. Williams, Phys. Rev. **79**, 1007 (1950).
14. K. P. R. Nair, J. Hoeft and E. Tiemann, Chem. Phys. Lett. **58**, 153, (1978).
15. R. E. Willis and W. W. Clark, J. Chem. Phys. **72**, 4946 (1980).
16. J. L. Dunham, Phys. Rev. **41**, 721 (1932).

17. W. H. Flygare and W. D. Gwinn, J. Chem. Phys. **36**, 787 (1962).
18. R. F. Curl and J. L. Kinsey, J. Chem. Phys. **35**, 1758 (1961).
19. J. Bardeen and C. H. Townes, Phys. Rev. **73**, 97 (1948); also Phys. Rev. **73**, 627 (1948).
20. H. S. Luftman, Ph.D. Thesis, University of California at Berkeley (1982).
21. F. J. Lovas and E. Tiemann, J. Phys. Chem. Ref. Data **3**, 609 (1974).
22. We have also obtained hyperfine spectra of ClF which contain transitions which may be attributed to higher J levels. Lowered source temperatures and/or increased pressures may be in order if unambiguous spectra are to be obtained.
23. C. H. Townes and A. L. Schawlow, Microwave Spectroscopy (McGraw-Hill, New York, 1955).

Chapter III.

"Van der Waals" Molecules and Deflection Experiments

Introduction

During the past decade, weakly-bound molecular species have been the subjects of numerous experimental and theoretical investigations, the results of which have been collected into several reviews.¹⁻³ The term weakly-bound, for the purposes of this discussion, is defined to include neon dimer (Ne_2 , $D_e = 29.7 \text{ cm}^{-1}$),⁴ xenon fluoride (XeF , $D_e = 1175 \text{ cm}^{-1}$),⁵ and the many atom-atom, atom-molecule, and molecule-molecule complexes with dissociation energies, D_e , between these extremes. A thorough understanding of the interactions which produce these simple "pseudomolecules" is essential to the theories of catalysis, nucleation, kinetics, atmospheric chemistry, and bulk properties of gases.

It had long been held that the intermolecular forces giving rise to weakly-bound species were electrostatic, rather than chemical, in nature. These forces were usually described in terms of induction, atom-atom additive pair potentials, and permanent electric moment interactions, rather than in the chemical terms reserved for the stronger bonding interactions that lead to "real" molecules. The experimental evidence of the past ten years has forced the revision, if not the outright abandonment of that theory for polyatomic species. A suitable replacement has not yet been

found, and it is unlikely that any one simple theory will propose to describe all of the observed molecular varieties which can be considered weakly-bound. As more experimental data on these new molecules are obtained, patterns of interaction will emerge; and theories consistent with these patterns will be advanced. Some of these will withstand experimental scrutiny; others will fail--exactly as has been the case with theories which describe "regular" molecules.

Klemperer^{2,6} and coworkers were among the first to point out the inadequacies of the electrostatic model for weak bonding in polyatomics. In a series of molecular beam electric deflection⁷⁻¹⁰ experiments, they determined that the polarities of many weakly-bound complexes were inconsistent with the geometries predicted by electrostatic theory. Through a series of molecular beam electric resonance experiments they determined the average, and estimated the equilibrium, structures and dipole moments of the complexes Ar-X (X= HF, HCl, ClF, OCS, CO₂, BF₃) and HF-X (X= HF, HCl, ClF).¹¹ The structures and dipole moments determined were entirely inconsistent with the predictions of electrostatic theory, but were highly suggestive of chemical bonding. The angular rigidity of the ClF complexes,¹²⁻¹⁴ and the anti-hydrogen bonded structure of HF-ClF¹⁴ were particularly provocative. The group suggested an elegantly simple explanation for their findings. They proposed that the weak bond results from a Lewis acid/base interaction between the highest occupied molecular orbital

(HOMO) of the donor and the lowest unoccupied molecular orbital (LUMO) of the acceptor.^{12,13} They also pointed out a correlation between the structures of gas phase complexes and the orientations of the components, relative to their nearest nonbonded neighbors, in the solid phase.^{8,9,12} These two simple pictures accurately predicted (in retrospect) the structures and/or polarities of all known polyatomic weakly-bound species.

Experiments

We proposed to test the theory of chemical interactions in weakly bound species by obtaining the radiofrequency spectra of $(\text{ClF})_2$ and Ar_2ClF . Molecular beam electric resonance spectroscopy has long been a method of choice for the study of weak molecular complexes. Virtually any desired species can be synthesized in a nozzle expansion under carefully controlled (albeit empirically determined) source conditions.

Source conditions for electric resonance spectroscopy of loosely-bonded molecules are always compromises between requirements that exactly oppose one another. Low source temperatures and high nozzle backing pressures enhance cluster formation, but the resulting molecules may be so rotationally cold that they cannot be refocussed. ($J=0$ states have a negative Stark effect, and are always defocussed.) Higher source temperatures and lower pressures favor increased transmission, but at the expense of overall

signal intensity. While the source conditions that provide the maximum in refocussed beam intensity are a good starting point, true source optimization can only be done on-resonance after a transition has been located.

The data presented in this chapter were collected during the determination of source conditions for $(\text{ClF})_2$. Although resonance spectra have not yet been obtained, the mass spectra and refocussing data contain a great deal of qualitative information about the molecular species present in the beam.

Experiments were performed at a variety of source temperature and pressure combinations ranging from 293 K and 760 torr to 370 K and 3200 torr. The nozzle, stopwire, and detector aperture diameters were 0.010 cm, 0.090 cm, and 0.152 cm, respectively. Source to stopwire and stopwire to detector distances were 42.6 cm and 61.4 cm. The gas mixture used was 3% ClF in argon and was prepared by filling an evacuated cylinder to the desired ClF partial pressure, then pressurizing to 100 P_{SiG}. The ClF was obtained from the Ozark Mahoning Company and was used without further purification.

Mass spectra from 50 to 190 amu were recorded at each set of source conditions with the fields turned off and no obstacles in the beam, with the fields turned off and the stopwire positioned so that the signal at $m/e=54$ (Cl^{35}F^+) was minimized, and with the stopwire in place and the A field turned to 24 kilovolts. Intensities were measured as

peak heights above the background established with the stopwire in. Occasionally, spectra were recorded with the field on and the stopwire out, and the signal enhancement over the straight-through beam with no field was recorded. Measurements of this sort provide useful indications of polarity in regions where the background is high and the percent refocussing is small.

Figure III-1 shows a mass spectrum recorded at 293 K and 1900 torr. Background peaks are from the thoriated tungsten ionizer filament. Table III-1 lists the mass to charge ratios and identities of halogen containing ions monitored during this study. Where several isotopes are possible, the most abundant is(are) listed. Ions whose intensities are less than one percent of the Cl^{35}F^+ signal are not listed. Intensities and refocussing observed under three sets of source conditions are presented for comparison. While day-to-day signal fluctuations often make comparisons of absolute intensities unreliable, those reported here were reproduced over several consecutive days of experimentation. In each data set, the intensity of the $m/e=54$ peak is expressed in millivolts (recorded with a 10^9 ohm input resistance and particle multiplier voltage at 3.3 kV; this corresponds to a gain of 10^6), and the other peak intensities are expressed as fractions of that intensity.

Refocussing and/or signal enhancement due to the quadrupole field was observed, under varying source conditions, for all halogen-containing species in the beam.

Figure III-1

Mass spectrum, showing ClF clusters and fragments, of 3% ClF in argon at 293 K and 1900 torr. The underlying trace is background from the thoriated tungsten ionizer filament.

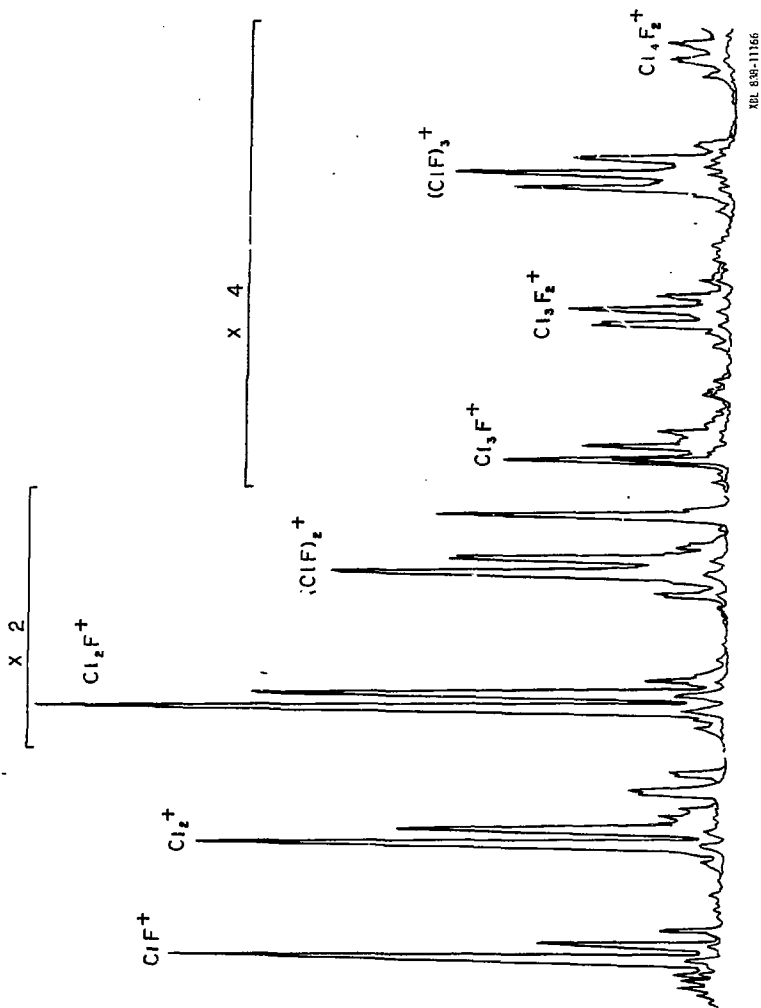


Table III-1

Comparison of Intensities and Refocussing for Halogen-Containing Species at Different Source Conditions

m/e	Species	Intensity* (Percent Refocussing)		
		293K/1900 torr	317K/1900 torr	369K/2050 torr
54	ClF ⁺	1450 mV (28.3)	1200 mV (91.2)	500 mV (210)
70	Cl ₂ ⁺	0.946 (3.45)	0.425 (13.1)	0.302 (17.1)
89	Cl ₂ F ⁺	0.614 (1.77)	0.251 (12.3)	0.125 (35.4)
94	ArClF ⁺	0.027 (70.0)	0.021 (69.2)	0.043 (48.1)
108	(ClF) ₂ ⁺	0.356 (5.34)	0.235 (15.3)	0.260 (25.0)
124	Cl ₃ F ⁺	0.050	0.027	---
126		0.056	0.029	0.013
143	Cl ₃ F ₂ ⁺	0.063	0.018	---
145		0.067	0.022	---
159	Cl ₄ F ⁺	0.031	---	---
162	(ClF) ₃ ⁺	0.092	0.104	0.043
164		0.121	0.118	0.068
180	Cl ₄ F ₂ ⁺	0.026	0.015	0.016

* Intensities of other ions are ratioed to ClF⁺. Only most abundant isotopes with intensities of 0.010 or greater are listed.

The higher mass clusters did not, however, exhibit significant refocussing in the spectra selected for the table.

Figures III-2, 3, and 4 show refocussing observed for $m/e=108$ and 89, 70, 145 and 162 at 350 K and 2200 torr.

A number of authors¹⁵ have shown that logarithmic plots of transmittance (or percent refocussing) versus lens voltage yield qualitative information about molecular geometries and dipole moments. Quantitative information may be obtained by comparing the refocussing behavior of the species in question to that of a known similar molecule under the same experimental conditions. Figure III-5 shows logarithmic plots of transmittance versus voltage for OCS and ClF.¹⁶ Both gases were 5% in argon, and were expanded through 100 micron nozzles at 293 K and 760 torr. Figure III-6 shows similar plots of the refocussing behavior observed by monitoring $m/e=108$, 89, and 70. These data were obtained at 350 K and 2200 torr. Figure III-7 shows plots of refocussing observed for ClF¹⁶ and for the $m/e=70$ species at 293 K and 1600 torr.

Analysis: ClF Clusters

In earlier deflection studies Bowen¹⁰ observed refocussing comparable to what we report for ClF dimer, and no refocussing for the trimer. He proposed a symmetric six-membered ringlike structure for the nonpolar trimer, and an L-shaped structure analogous to that proposed for chlorine dimer,⁹ $(Cl_2)_2$, for the dimer. Although he did not specify,

Figure III-2

Refocussing observed while monitoring the signals at $m/e=108$ ($(Cl^{35}F)_2^+$) and 89 ($Cl^{35}_2F^+$). Steps indicate 2.7 kilovolt increments in the A field voltage. These data were recorded at 350 K and 2200 torr.

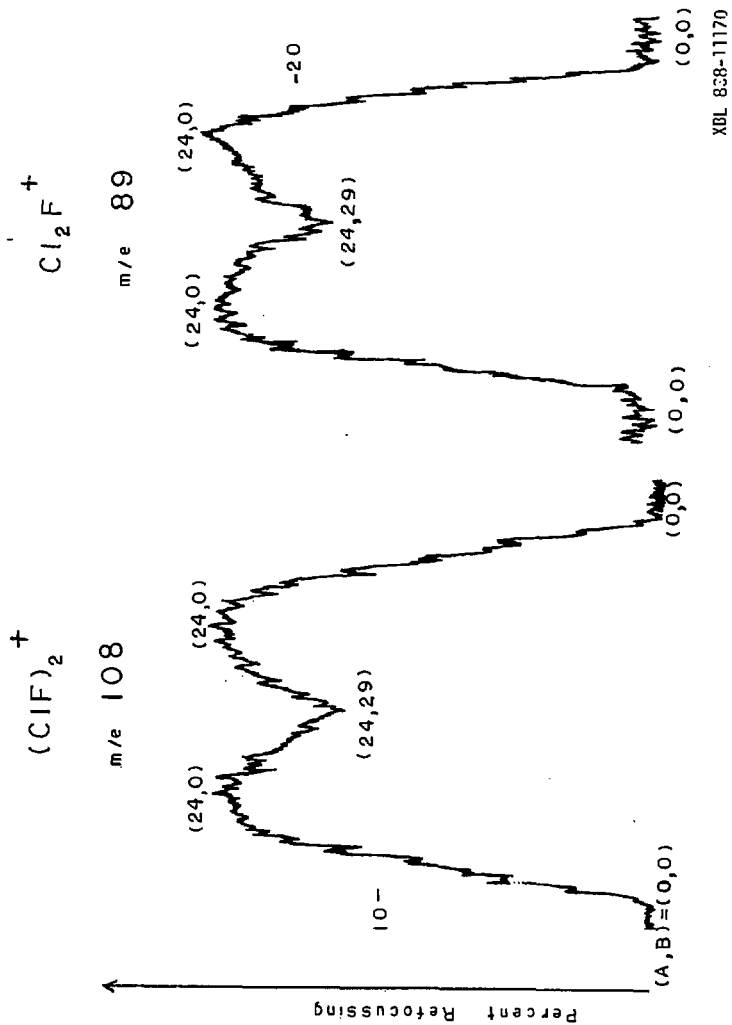


Figure III-3

Refocussing observed while monitoring the signal at $m/e=70$ ($\text{Cl}^{35}_2^+$). Steps indicate 2.7 kilovolt increments in the A field voltage. These data were obtained at 350 K, and 2200 torr.

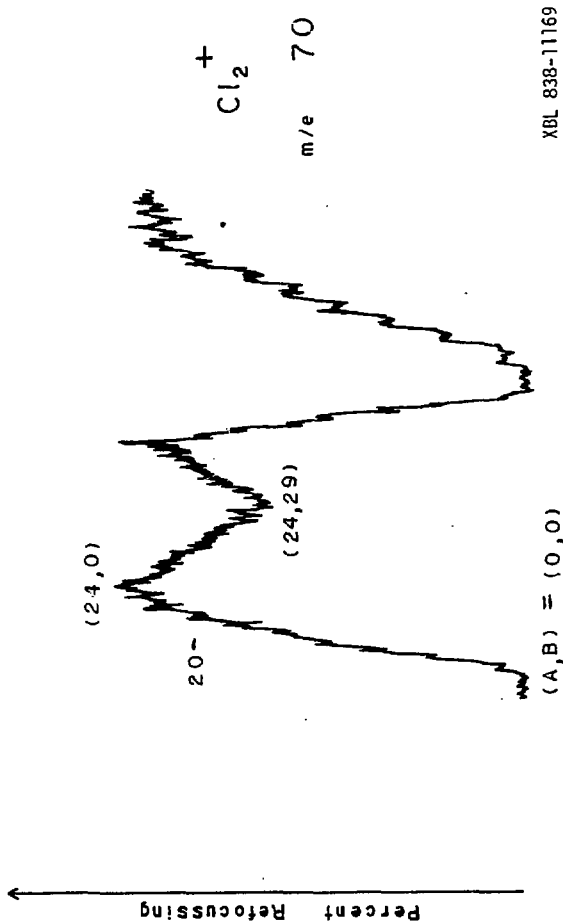
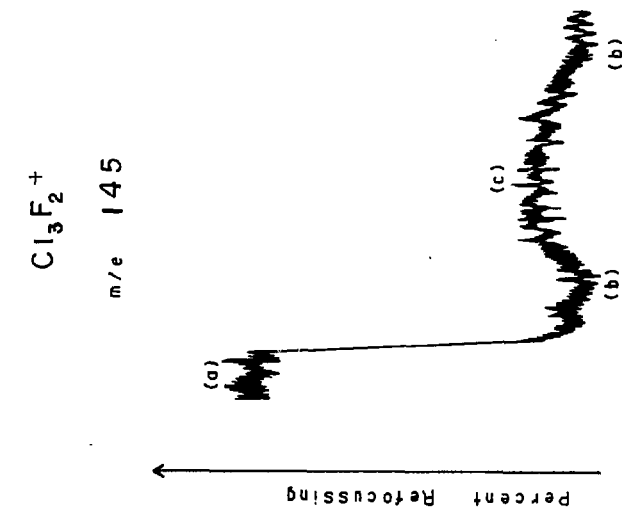
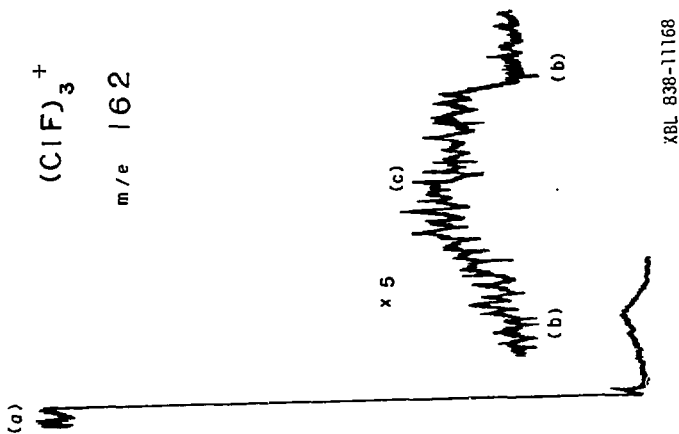


Figure III-4

Refocussing observed while monitoring the signals at $m/e=145$

($Cl_3F_2^+$) and 162 ($(ClF)_3^+$) at 370 K and 2200 torr:

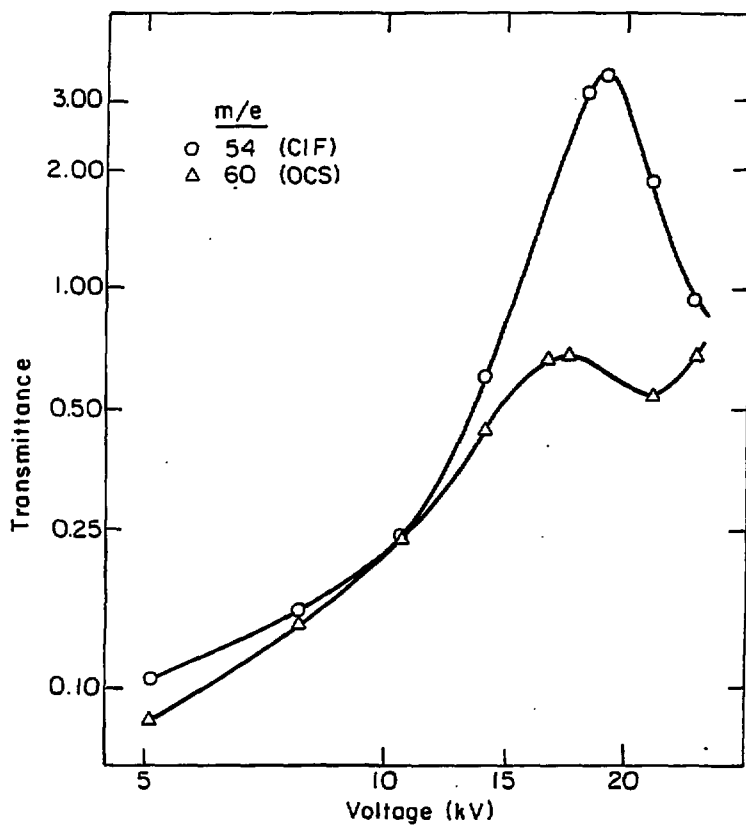
- (a) straight-through beam, no fields
- (b) stopwire in, no fields
- (c) stopwire in, A field at 24 kV.



XBL 838-11168

Figure III-5

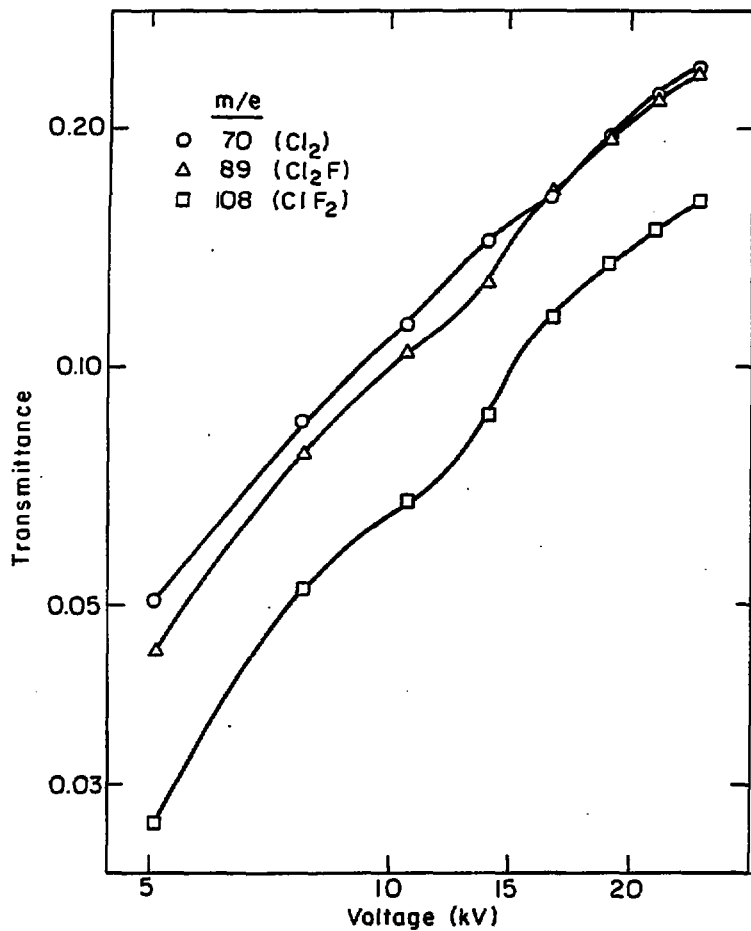
Log transmittance versus log voltage plotted for OCS and ClF at 293 K and 760 torr. The greater ClF transmittance is attributed to a greater population in the $J=1$ state under these source conditions.



XBL 838-6221

Figure III-6

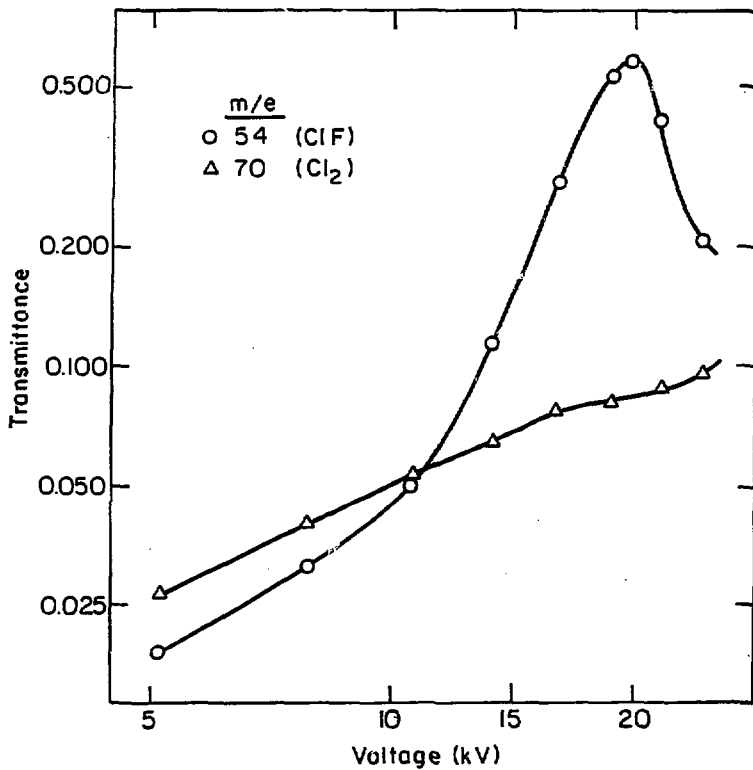
Log refocussing versus log voltage observed at $m/e=108$
($(ClF)_2^+$), 89 (Cl_2F^+), and 70 (Cl_2^+). The similarity
of the curves indicates that Cl_2F^+ and Cl_2^+ are fragments of
ClF dimer.



XBL 638-6220

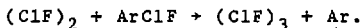
Figure III-7

Log refocussing versus log voltage for $m/e=70$ (Cl_2^+)
compared to that of $m/e=54$ (ClF^+) under the same source
conditions.



XBL 836-6222

one must assume the intended atomic arrangement in the dimer was ClF-ClF, as is shown in Figure III-8. That assumption is based on the theory that the trimer is formed without rearrangement from the dimer in reactions such as



The extremely low intensities of argon-containing clusters in the mass spectra of mixtures rich (one percent or greater) in ClF are attributed to the exothermicity of these reactions.

The proposed dimer structure is inconsistent with the mass spectral and refocussing data and, incidentally, with the HOMO/LUMO model which Bowen and coworkers claim to support. The rotational constants for the geometry shown are: A = 16663 MHz, B = 1135 MHz, C = 1063 MHz. The dipole moment determined by projecting the individual ClF moments¹⁷ onto the a axis is 1.10 Debye. Widening the bond angle from the 90° shown increases the dipole moment. Any geometry similar to that of Figure III-8 yields the same result: a near-prolate asymmetric top with a dipole moment component along the a axis greater than the dipole moment of ClF itself. In other words, this is a molecule which should refocus strongly.¹⁹ Our data, recorded at several temperatures and pressures, indicate that it does not.

It is well known that fluorine containing molecules fragment under electron bombardment, producing daughter ions with fewer fluorines than the parent. (Sometimes the parent itself is not observed.) ClF dimer, on electron bombardment

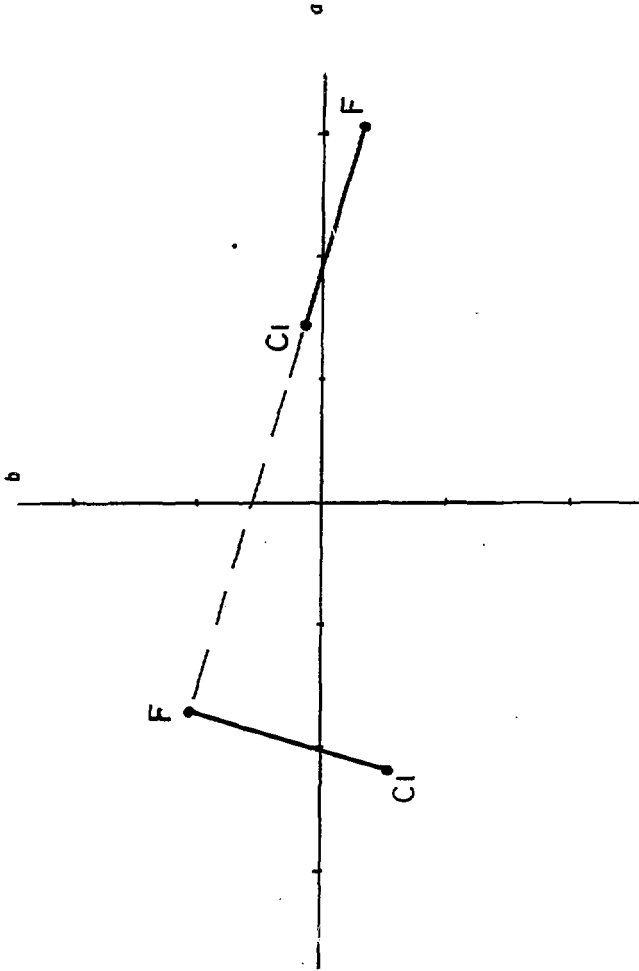
Figure III-8

Previously proposed geometry for ClF dimer. Cl-F-Cl bond angle is 90° . Individual ClF units have 1.63 bond lengths. The weak bond is shown 3.34 Å long.¹⁸

Rotational Constants (MHz) are: A = 16663
B = 1135
C = 1063

The a inertial axis is rotated 16.3° from the FCl-F bond. The dipole moment component along the a axis is $\mu_a = 1.10$ Debye.

Ray's asymmetry parameter for the structure is -0.991.



XBL 838-11167

in our ionizer, yields ions at mass to charge ratios corresponding to the parent, $(ClF)_2^+$, and the fragments Cl_2F^+ and Cl_2^+ . While ClF mixtures are usually contaminated with some chlorine, most of the intensity we observe at $m/e=70$ is not from chlorine in the original mixture. Cl_2 itself is nonpolar, but we observe an intense peak which tracks the cluster peaks' intensities in the mass spectra, and which gives the same refocussing pattern we observe at $m/e=108$ and 89 . This Cl_2^+ must be a fragment of ClF dimer, and it is unlikely that Bowen's proposed geometry could yield this fragment in such intensity.

Finally, Bowen's geometry is inconsistent with the HOMO/LUMO model which he and his coworkers advanced. In ClF, both the $p\pi^*$ HOMO and the po^* LUMO are associated primarily with the chlorine atom. The model would dictate a geometry similar to Bowen's, but with the chlorine atoms together. This is the geometry we propose, and it is shown in figure III-9. Our structure is also a near-prolate asymmetric top, but its dipole moment along the a axis is only 0.32 Debye. Bowen proposed an analogous structure, with the iodine atoms together, for ICl dimer. As he pointed out, nearest neighbor units in crystalline ICl have a similar arrangement.^{20,21} The crystal structure of ClF is not known.

The structure we propose for ClF dimer cannot lead to a symmetric six-membered ringlike trimer. Given the refocussing we observe at $m/e=162$ and 145 , it is questionable

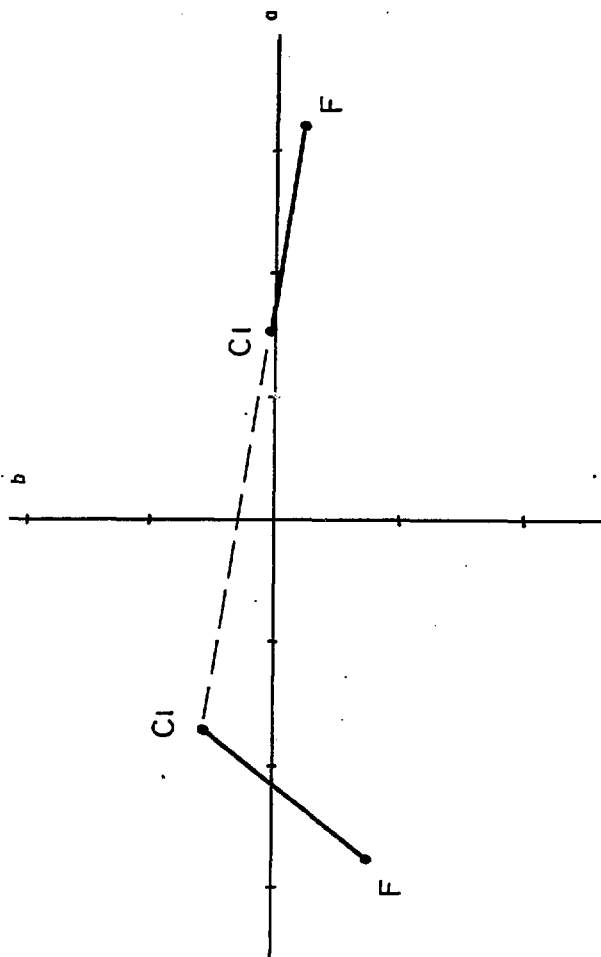
Figure III-9

ClF dimer structure proposed in this work. The Cl-Cl-F bond angle is 120° . Individual ClF bond lengths are unperturbed. The weak bond is 3.34 Å long.

Rotational constants (MHz) are: A = 24669
B = 1022
C = 981

The a inertial axis is rotated 8.65° from the FCl-Cl bond.
 $\mu_a = 0.32$ Debye.

Ray's asymmetry parameter for this geometry is -0.997.

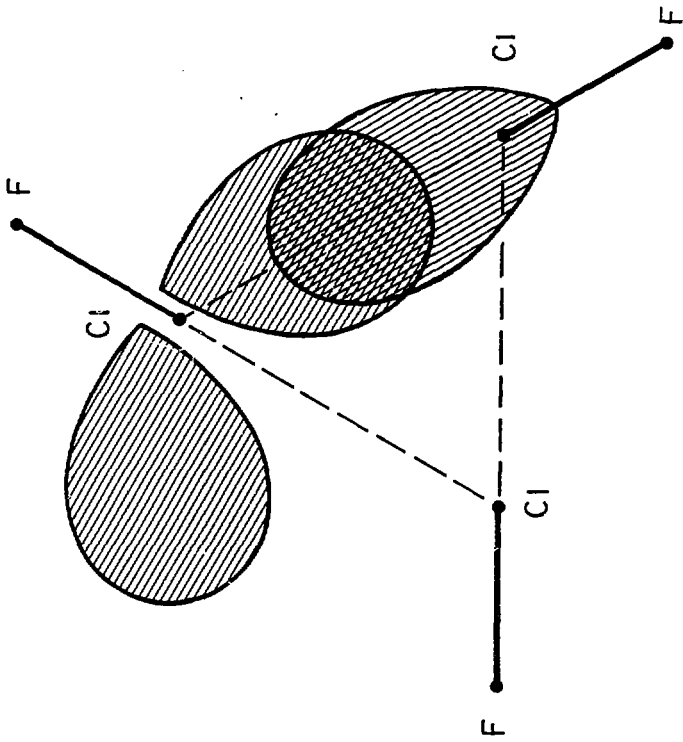


XBL 838-11164

whether a nonpolar geometry is appropriate. For ICl trimer, which was observed to refocus slightly, Bowen suggested an asymmetric six-membered ring. While such a geometry for ClF trimer might explain the observed refocussing, it represents a rather sudden departure from the guidelines we have followed in predicting the dimer structure. If we use those guidelines again, we obtain the interesting trimer geometry shown in Figure III-10.²² This planar structure is nonpolar in the ground vibrational state²³ and yields the Cl₃ cluster-containing fragment ions indicated by the mass spectral data. While several chainlike structures provide the same amount of HOMO/LUMO overlap, none of those are nonpolar. We suggest that the refocussing we observe may be due to ClF tetramer, rather than to ClF trimer. Our proposed trimer structure leads to an obvious tetramer geometry. A fourth ClF could overlap its LUMO with the degenerate HOMOs located above and below the trimer plane, forming a pyramidal symmetric top. Again, our proposed structure yields fragment ions consistent with the observed mass spectra. Its dipole moment is just that of ClF monomer if the trimer remains planar and is zero if all three fluorines are distorted by 30° from the plane. It would be very informative and rather easy to extend the mass spectrum to the tetramer parent ion at m/e=216 and to compare the refocussing of this ion to that of a known symmetric top of similar mass, such as CCl₃Br or CCl₃I.

Figure III-10

Nonpolar ClF trimer geometry proposed in this work. The HOMO/LUMO overlap for one of the Cl-Cl bonds is indicated. All FCl-Cl-F bond angles are 120° . ClF and Cl-Cl bond lengths are 1.63 Å and 3.34 Å, respectively.



XBL 838-11165

Analysis: Ar₂ClF and Ar₃ClF

Although the gas mixture used in these experiments was too rich in ClF to produce substantial quantities of the argon containing clusters, weak features in the mass spectrum were observed at $m/e=174$, 155, 134, and 115, which correspond to Ar₃ClF⁺, Ar₃Cl⁺, Ar₂ClF⁺, and Ar₂Cl⁺. These features rarely appeared in the straight-through beam, but grew when the fields were turned on. This indicates that these species, while present in very small quantities, are strongly refocussing. Given the structure and refocussing characteristics of ArClF, this is hardly surprising. Argon containing clusters are formed by reactions such as



and it seems clear that the argon cluster must bond to the chlorine end of the ClF molecule. Harris¹² and coworkers remarked that the HOMO/LUMO theory, after accurately predicting the geometry of ArClF, left the structure of Ar₂ClF completely unresolved. While the addition of a second argon atom to an ArClF cluster is difficult to conceptualize, bonding between argon dimer, a rather structureless Lewis base, and the ClF molecule presents a straightforward picture. The geometry which provides the maximum overlap with the ClF LUMO is a Y-shaped C_{2v} structure, which should be strongly refocussing since it has the dipole moment of ArClF and a smaller rotational constant. Similar considerations lead to a symmetric top geometry, also strongly refocussing, for Ar₃ClF. A mixture

of approximately 0.2 percent ClF in argon and a source pressure of 1500-2000 torr should produce these molecules in quantities adequate for the spectroscopic experiments needed to determine their structures accurately.

Conclusions

Mass spectral and refocussing data alone cannot provide the exact molecular information needed to determine molecular structures, but can be used to sort structural possibilities. The data obtained in this preliminary investigation are suggestive of cluster geometries which are most easily explained in chemical terms. The HOMO/LUMO interaction model predicts structures which, at this point, are consistent with our observations. That the structures predicted for dimers are similar to orientations in known crystal structures, we suspect, is no accident. Since clusters have no need for long-range order, the likeness need not extend to trimers and other larger clusters. It is not yet known how many molecules are required for the transition from simple cluster geometry to ordered crystal symmetry to take place.

References for Chapter III

1. G. E. Ewing, *Acc. Chem. Res.* **8**, 185 (1975); G. E. Ewing, *Can. J. Phys.* **54**, 487 (1976); B. L. Blaney and G. E. Ewing, *Ann. Rev. Phys. Chem.* **27**, 553 (1976).
2. W. Klemperer, in Advances in Laser Chemistry, edited by A. H. Zewail (Springer-Verlag, Berlin, 1978); W. Klemperer, *J. Mol. Struct.* **59**, 161 (1980).
3. J. S. Winn, *Acc. Chem. Res.* **14**, 341 (1981).
4. C. Y. Ng, Y. T. Lee and J. A. Barker, *J. Chem Phys.* **61**, 1996 (1974).
5. P. C. Tellinghuisen, J. E. Velasco, J. A. Coxon, D. W. Setser, *J. Chem. Phys.* **68**, 5177 (1978).
6. J. M. Deutch and W. Klemperer, *J. Chem. Phys.* **66**, 2753 (1977).
7. T. R. Dyke, W. Klemperer, A. P. Ginsberg, and W. E. Falconer, *J. Chem. Phys.* **56**, 3993 (1972).
8. S. E. Novick, P. B. Davies, T. R. Dyke, W. Klemperer, *J. Am. Chem. Soc.* **95**, 8547 (1973); S. E. Novick, J. M. Lehn and W. Klemperer, *J. Am. Chem. Soc.* **95**, 8189 (1973).
9. S. J. Harris, S. E. Novick, J. S. Winn, W. Klemperer, *J. Chem. Phys.* **61**, 3866 (1974).
10. K. Bowen, Ph.D. Thesis, Harvard University (1977).
11. This is a very incomplete list of the structures determined by this group. Specific references for many of the molecules listed are given in Reference 2.
12. S. J. Harris, S. E. Novick, W. Klemperer, and W. E. Falconer, *J. Chem. Phys.* **61**, 193 (1974).
13. S. E. Novick, S. J. Harris, K. C. Janda, and W. Klemperer, *Can. J. Phys.* **53**, 2007 (1975).
14. S. E. Novick, K. C. Janda and W. Klemperer, *J. Chem. Phys.* **65**, 5115 (1976).
15. See References 22-24 in Chapter I.
16. The ClF and OCS refocussing data were taken by H. S. Luftman.

17. The dipole moment of ClF is 0.8881 Debye; B. Fabricant and J. S. Muentzer, *J. Chem. Phys.* **66**, 5274 (1977).
18. From Reference 12, 3.33 Å is the Ar-Cl bond length in ArClF. In chlorine crystal, 3.34 Å is the distance between nearest nonbonded neighbors; R. L. Collins, *Acta. Cryst.* **5**, 431 (1952); S. W. Walmsley and A. Anderson, *Mol. Phys.* **7**, 401 (1964).
19. From Reference 12, the spectroscopic constants of ArClF are: $(B+C)/2 = 1327.113$ MHz, $\mu_a = 1.053$ Debye. We observe strong refocussing of ArClF in these experiments.
20. K. H. Boswijk, J. van der Heide, A. Vos, E. H. Wiebinga, *Acta. Cryst.* **9**, 274 (1956).
21. G. B. Carpenter and S. M. Richards, *Acta. Cryst.* **15**, 360 (1962).
22. This geometry was first proposed by D. Fox in a discussion with the author.
23. We suggest that we are observing tetramer fragments because similar refocussing is observed at higher masses. Our trimer, however, is refocussable if the doubly degenerate E' ring deformation is excited.

Appendix I.

C Field Recalibration

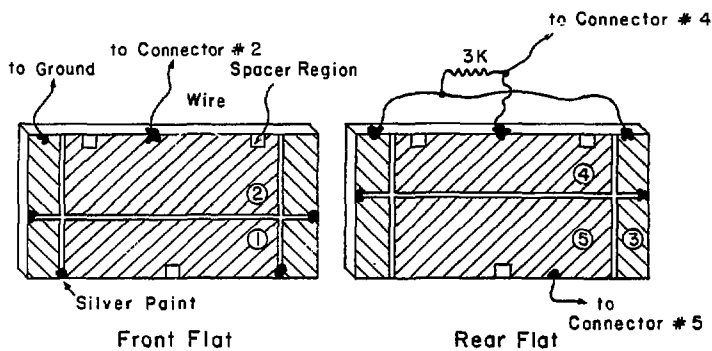
The spacing between our C field flats was reported as 0.9908 cm by Luftman.¹ This value was determined by fitting observed OCS J=1, M=0 \rightarrow 1 resonances to fourth order in the electric field. Obsolete values of the OCS molecular constants were inadvertently used in this fit.

The plate separation has been recalculated using Muentzer's more recent values² of the OCS spectroscopic constants. The equations given by Muentzer, which include contributions to the energy from second and fourth order Stark effects and from the field-induced electric dipole moment, were solved for the effective electric field strength at each experimental voltage/frequency point. The plate separation was calculated as the ratio of the measured voltage to the effective field strength. The average value obtained for the spacing was 0.99989 ± 0.00006 cm.

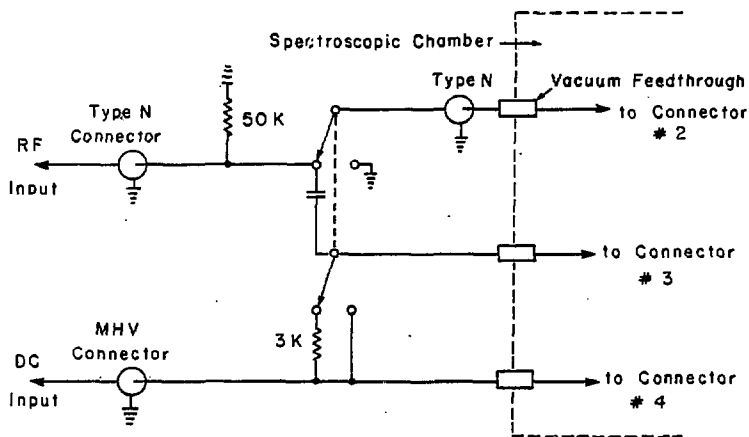
Figure AI-1 shows schematic drawings of the C field and its circuitry. Due to a printing error, these drawings were omitted from several copies of Luftman's work, where they were parts (b) and (c) of Figure 2.5 (p. 30).

Figure AI-1

Schematic drawings of the C field flats and of the circuitry used to deliver the static and oscillating electric fields to the resonance region.



(b) Gold Inner Surfaces of Flats



(c) C Field Electric Schematic

XBL 829-11414

References for Appendix I

1. H. S. Luftman, Ph.D. Thesis, University of California at Berkeley, 1982.
2. J. S. Muentner, J. Chem. Phys. 48, 4544 (1968).

Appendix II.

Computer Programs SINGLET SIGMA and TOPSPIN

The computer programs SINGLET SIGMA and TOPSPIN were used to calculate energy levels and transitions and to fit molecular constants to observed transitions. SINGLET SIGMA, which will be discussed briefly, is listed on microfiche which is affixed to the back cover. TOPSPIN will be discussed in more detail and is listed at the end of this appendix.

SINGLET SIGMA

This program was written by G.R. Tomasevich¹ and is well documented in his thesis. The program calculates hyperfine (not rotational) energy levels, transitions, and line strengths for linear molecules in singlet sigma electronic states. The Hamiltonian is forced to be block-diagonal in J; perturbation theory corrections to the matrix elements include the Stark effect through fourth order and the quadrupole interaction through second order. The calculation includes spin-rotation interactions, direct and electron-coupled spin-spin interactions, and field-induced dipole contributions to the Stark effect. Any or all of the molecular constants may be fitted to observed spectra by inputting the experimental lines and assignments, and a set of trial molecular constants. The program adjusts the constants, using an iterative linear least squares

algorithm, until the best agreement between the observed and calculated spectra is obtained.

The program was originally written in IBM 360 FORTRAN, and was rewritten for Berkeley's CDC 6600. Computations are in single-precision, which is equivalent to the double-precision used in the IBM version. Read error messages and other "safety features" included in the original were not included in the CDC version.

The major modification made by the author pertains to the calculation of second order quadrupolar energies. The original program calculates energy levels for molecules having one quadrupolar nucleus and one other nucleus with nonzero spin. Second order corrections, calculated by a separate program, were added to the matrix elements before diagonalization. The current version is capable of calculating energies for two quadrupolar nuclei. Second order corrections are added to the eigenvalues after diagonalization. For a single quadrupolar nucleus, the corrections have been tabulated by Townes and Schawlow.² For two quadrupolar nuclei, calculation of the corrections is somewhat more complicated and is as follows.

The eigenstates of the quadrupolar Hamiltonian may be labelled $|I_1 I_2 I J F\rangle$, where I_1 and I_2 are the individual nuclear spins, I is the total nuclear spin and is the vector sum of I_1 and I_2 , J is the rotational angular momentum, F is the total angular momentum and is the vector sum of I and J . In fact, I and J are not good quantum numbers. The

Hamiltonian has nonzero matrix elements for $I'=I, I\pm 1, I\pm 2$ and $J'=J, J\pm 2$. To first order in J the eigenstates are:

$$|IJF\rangle = \sum_{I'} a_{I'} a_{I'} |I'JF\rangle .$$

The second order energies are calculated from the first order eigenstates as:

$$E^{(2)}(I, J, F) = \sum_{J'} \sum_{I'} \frac{\langle "I"JF | H_Q | "I'"J'F \rangle}{E(I, J, F) - E(I', J', F)} ,$$

where the quotes remind us that the first order eigenstates are not true eigenfunctions of I , and the $E(I, J, F)$ are the first order energies. Expansion of the first order wavefunctions and substitution into this expression yield:

$$E^{(2)}(I, J, F) = \sum_{J'} \sum_{I'} \sum_{I''} \sum_{I'''} a_{II''}^* a_{II'''} \frac{\langle I''JF | H_Q | I'''J'F \rangle}{E(I, J, F) - E(I', J', F)} .$$

Formulas for the matrix elements of H_Q are given by Flygare and Gwinn³ and by Wollrab.⁴ Substitution of the matrix elements and first order eigenvectors into the above equation yields, after some arithmetic, a final expression of the form:

$$E^{(2)}("I", J, F) = \{ C_1(\text{eqQ1})^2 + C_2(\text{eqQ2})^2 + C_3(\text{eqQ1})(\text{eqQ2}) \} \div B$$

where B is the rotational constant. The C 's are the second order correction coefficients and are entered into the

program for each eigenvalue.

Because this program includes the smaller hyperfine terms and calculates line strengths, it is extremely useful for the analysis of high resolution molecular beam electric resonance spectra. Because it uses perturbation theory rather than a direct diagonalization of the Hamiltonian, it is relatively inexpensive to use. The strong field basis ($|M_1 M_2 M_J M_F\rangle$) used in the calculations is inconvenient for those who want to have some idea of how the calculations are done, but the program's major drawback is its limited applicability.

TOPSPIN

This program is a combination of the programs TWOQUAD and ASYM written by S. J. Harris.⁵ The programs were originally written for the IBM 360 and were merged when they were rewritten for the CDC 6600. TWOQUAD calculates rotational and hyperfine energies and transitions for symmetric tops (and linear molecules) with up to two quadrupolar nuclei, which must be located on the symmetry axis. Stark effects and centrifugal distortion are included in the calculations; spin-rotation and spin-spin interactions are not. ASYM calculates rotational energies and transitions, including the Stark effect, for asymmetric tops with one or two dipole moment components. It does not consider centrifugal distortion or hyperfine effects. The combination program retains the capabilities of the

originals. Calculation of hyperfine levels for very asymmetric tops is not guaranteed to give reasonable results.

The program calculates matrix elements in the basis $|I_1 I_2 IJKF_M\rangle$, where K is the component of rotational angular momentum along the molecular symmetry axis, and the other quantum numbers have the meanings already discussed. The energy matrix is truncated at J plus and minus two above and below the highest and lowest J of interest. The quadrupole matrix elements are calculated exactly in zero field. Tomasevich's line fitting subroutine was modified and added to the program so that molecular constants could be fitted to as many as five sets of spectra. The data sets may have different values of the electric field strength, but must have the same J. Inputs to TOPSPIN are discussed in the following paragraphs.

IFLAG1,IFLAG2,IFLAG3,IFLAG4,IFLAG5,IFLAG6,NFIT

The IFLAGs control the output. IFLAG1=0 prints all nonzero matrix elements, IFLAG1>0 ignores this. IFLAG2=0 prints the coefficients of the eigenvectors. If IFLAG3=0 also, all of the coefficients are printed; IFLAG3>0 prints only the coefficients whose squares are larger than 0.2. No coefficients are printed for IFLAG2>0. IFLAG4=0 prints eigenvalues. IFLAG5=0 prints quantum numbers and diagonal matrix elements. IFLAG6=0 prints the frequency derivative matrix calculated during the fit. During line fitting, all

these outputs are printed at the end of each program cycle. NFIT is the number of data sets to be included in the line fitting. The current limit is five data sets; this can be changed by changing the dimension statements.

IDELMF, IDELJ, IDELF, IDELK, IDELI, NTOT, NPAR

The IDELS are selection rules used by the program in calculating transitions. Only transitions having $\Delta X < IDELX$ are retained. NTOT is the maximum number of program cycles allowed during line fitting. NPAR is the number of molecular parameters to be varied in the fitting.

FRMIN, FRMAX

These are the minimum and maximum transition frequencies, in kHz, retained by the program.

JJJ, KKK, XI1, XI2

JJJ is the lower J of interest for rotational transitions or the J of interest for hyperfine transitions. KKK is the K of interest for symmetric tops. Enter 0 for linear molecules and asymmetric tops. XI1 and XI2 are the nuclear spins. The program does not believe in spin-rotation interactions, so do not enter 0.50.

PAR(I), I=1,7

These are the molecular constants available for fitting. In order, they are: A, B, C the rotational

constants in kHz. For linear molecules, $A=0.0$. For symmetric and near-symmetric asymmetric tops, A is the rotational constant for the symmetry axis. $EQQ1, EQQ2$ are the nuclear quadrupole coupling constants in kHz. If $EQQ1=0.0$, the program does not calculate quadrupole matrix elements. AMU, BMU are the dipole moment components, in Debye, along the A and B axes. A is the symmetry axis. BMU is 0.0 for symmetric tops and linear molecules.

DJ,DK,DJK

These are the centrifugal distortion coefficients in kHz. The last two are 0.0 for linear molecules. The program does not realize that asymmetric tops have centrifugal distortion effects, so the coefficients should all be zero or strange numbers may result.

The following inputs apply only to line fitting.

NPT(I),E(I), I=1,NFIT

$NPT(I)$ is the number of experimental lines in data set I . The current limit is 200 transitions per data set. $E(I)$ is the electric field strength in volts/cm.

I1,I2,FREQ(I), I=1,NPT

$I1$ and $I2$ are the labels which assign the transition. You have to run the program to find out which state labels refer to which quantum numbers. $FREQ$ is the observed.

transition frequency in kHz. The transitions and their labels should be arranged in descending order, one to a line. After the last transition for data set 1, start over with NPT(2),E(2), etc. until all NFIT data sets are entered.

NORD(I),DELA(I), I=1,NPAR

The NORDs tell the program which molecular parameters are to be fitted and in what order. NORD(3)=5, for example, means that EQQ2 is to be the third varied parameter. DELA(I) is the amount by which PAR(I) is incremented during the first program cycle.

DELFO

The last input for line fitting is DELFO, the average frequency change in kHz, that you wish to accomplish in each program cycle. After the first cycle, the DELAs are adjusted so that this average change is achieved. Current parameter values are printed on each pass through the program. Transition frequencies and other output are printed at the end of each complete cycle.

If fitting is not desired, the last input is E, the electric field strength. Any number of E values may be entered, one to a line. The program stops when it reads a negative E value or when it runs out of data.

This program currently calculates energies and transitions in kHz. Changing the Stark effect constant from 503.4036 to 0.5024036 and inputting the molecular constants in MHz changes the output to MHz.

A final note of caution: due to the direct diagonalization procedure, this is an expensive program. It is not "idiot proof," so you should know what you are doing and should have some idea of what results you expect.

The program listing follows.

```

PROGRAM TOPSPIN(INPUT,OUTPUT,TAPE5=INPUT,TAPE6=OUTPUT)
COMMON/SXJCOM/QJ1,QJ2,QJ3,QL1,QL2,QL3,Q
COMMON/CLBCOM/WL1,WL2,WL,WM,WN,W
COMMON/FITCOM/FREQ(200,5),FCALC(200,5),DERIV(200,5,7),
IAO(7),DELA(7),D(7,8),LCALC(200,5),NORD(7),IDEN(200,5),
ZNPT(5),E(5),A,B,C,EQQ1,EQQ2,AMU,BMU,CONST,DELFQ,
3I5,ICYC,IDAT,IFLAG6,ILL,IFM1,INCR,JLST,LSTSQ,
4MPAR,NPAR,NFIT,NTOT,STDV,STDVP
COMMON/BIGCOM/HAMIL(5000),DEIGEN(10000),EIG(1000)
COMMON FACT(20)
INTEGER FBOT,FTOP,F,FPBOT,FPTOP,FP,DIAG,COUNT
DIMENSION PAR(7)
DIMENSION YMF(1000),YJ(1000),YF(1000),YK(1000),YI(1000)
EQUIVALENCE (A,PAR(1))

```

C

```

FACT(1)=1.0
DO 11 N=1,19
FACT(N+1)=N*FACT(N)
11 CONTINUE
READ(5,1010) IFLAG1,IFLAG2,IFLAG3,IFLAG4,IFLAG5,IFLAG6,NFIT
1010 FORMAT(7I5)
READ(5,1010) IDELMF,IDELEJ,IDELEF,IDELEK,IDELEI,NTOT,NPAR
READ(5,1020) FRMIN,FRMAX
1020 FORMAT(2F15.4)
READ(5,1030) JJJ,KKK,XI1,XI2
1030 FORMAT(2I5,3F4.1)
READ(5,1040) (PAR(I),I=1,7)
1040 FORMAT(F15.8)
READ(5,1050) DJ,DK,DJK
1050 FORMAT(3F15.8)
IF (NFIT.EQ.0) GOTO 85
DO 50 I=1,7
NORD(I)=8
DO 50 J=1,5
DO 50 K=1,200
50 DERIV(K,J,I)=0.0
DO 70 I=1,NFIT
READ(5,1060) NPT(I),E(I)
1060 FORMAT(I5,F15.8)
NP=NPT(I)
DO 60 J=1,NP
READ(5,1070) I1,I2,FREQ(J,I)
1070 FORMAT(2I5,F15.8)
60 IDEN(J,I)=65536*I1+I2
70 CONTINUE
READ(5,1080) (NORD(I),DELA(I),I=1,NPAR)
1080 FORMAT(I1,1X,F15.8)
READ(5,1040) DELFQ
STDVP=0.0 $ ISTSQ=0 $ I5=0
INCR=1 $ ILL=1 $ ICYC=1
GOTO 90
85 IDAT=1
READ(5,1040) E(IDAT)
IF (E(IDAT).LT.0.0) GOTO 999

```



```

GOTO 100
90 I5=I5+1
DO 900 IDAT=1,NFIT
WRITE(6,2000) I5,LSTSQ,IDAT
2000 FORMAT(//,10X,*TRIAL*,I5,*, PARAMETER*,I3,
1* BEING VARIED IN DATA SET*,I3)
100 BEFF=(B+C)/2
IF (A.EQ.0.0) BEFF=B
WRITE(6,2010) JJJ,XI1,XI2,E(IDAT)
2010 FORMAT(//,5X,*THIS RUN FOR J=*,I5,*, I1=*,F4.1,
1*, I2=*,F4.1,*, AND E=*,1PE15.8,* VOLTS/CM*)
IF (A.EQ.0.0) GOTO 115
WRITE(6,2020) A,B,C
2020 FORMAT(/,2X,*A(KHZ)=*,1PE15.8,*, B=*,1PE15.8,
1*, C=*,1PE15.8)
WRITE(6,2030) EQQ1,EQQ2,AMU,BMU
2030 FORMAT(/,2X,*EQQ1(KHZ)=*,1PE15.8,*, EQQ2=*,1PE15.8,
1*, AMU(DEBYE)=*,E15.8,*, BMU=*,E15.8)
GOTO 125
115 WRITE(6,2040) B,EQQ1,EQQ2,AMU
2040 FORMAT(/,2X,*B(KHZ)=*,1PE15.8,*, EQQ1=*,1PE15.8,
1*, EQQ2=*,1PE15.8,*, MU(DEBYE)=*,E15.8)
125 CONTINUE
JCOUNT=0 $ JCONT=0 $ LCOUNT=0 $ MCOUNT=0 $ LABEL=0
LSTART=1 $ LL=1
300 XMFBIG=JJJ+IDELJ+XI1+XI2
MFBIG=10.*XMFBIG+1.
MFTOP=MFBIG
XMFBOT=0.0
CHECK=2.*(XI1+XI2)
IF (AMOD(CHECK,2.0).EQ.1.0) XMFBOT=0.5
MFBOT=10.*XMFBOT+1.
DO 1 MF=MFBOT,MFTOP,10
IF (E(IDAT).EQ.0.0) MFTOP=MFBOT
IF (E(IDAT).NE.0.0.AND.A.NE.0.0) MFBOT=-MFTOP
DO 310 ISET=1,5000
HAMIL(ISET)=0.0
310 CONTINUE
C
IF (LSTSQ.GT.0) GOTO 330
IF (IFLAG1.GT.0) GO TO 319
WRITE(6,312)
312 FORMAT( ,*HERE ARE ALL THE NON-ZERO MATRIX ELEMENTS YOU ASKED
IFOR*,//)
WRITE(6,315)
315 FORMAT(///,5X,*MF*,6X,*J*,6X,*F*,6X,*K*,6X,*I*,12X,*J***,6X,
1*F***,6X,*K***,6X,*I***,10X,*KVECT*,8X,*HAMIL(KVECT)*,//)
GO TO 330
319 IF (IFLAG5.GT.0) GOTO 330
WRITE(6,320)
320 FORMAT(///,2X,*DIAGONAL ELEMENTS (FIRST ORDER PERTURBATION)?*)
WRITE(6,325)
325 FORMAT(///,4X,*MF*,6X,*J*,6X,*F*,6X,*K*,6X,*I*,10X,
1*ROW*,6X,*COL*,7X,*FIRST ORDER*,12X,*IDNO*,//)

```

C

```

330 IN=2 $ INIC=1 $ DIAG=1 $ LROW=0
    XMF=(MF-1.0)/10.0
    IF (A.NE.0.0.AND.E(IDAT).NE.0.0) XMF=(MF+1.)/10.
    XJTOP=JJJ+IDELJ+2.0
    JTOP=XJTOP+1.
340 XJBOT=AMAX1(FLOAT(JJJ-2),ABS(XMF)-XII-XI2,0.0)
    JBOT=XJBOT+1.
    DO 2 JJ=JBOT,JTOP
    XJ=JJ-1.0
    XFTOP=AMAX1(XJ+XII+XI2,ABS(XMF))
    FTOP=10.0*XFTOP+1.0
    XBIG=AMAX1(XII,XI2,XJ)
    XFBOT=AMAX1(ABS(XMF),2.0*XBIG-XJ-XII-XI2)
    FBOT=10.0*XFBOT+1.0
    DO 3 F=FBOT,FTOP,10
    XF=(F-1.0)/10.0
    KTOP=2.0*JJ-1.
    IF (A.EQ.0.0) KTOP=1
    IF (KKK.NE.0) KTOP=1
    KBOT=1
    DO 4 KK=KBOT,KTOP
    XK=(KK-JJ)
    IF (A.EQ.0.0) XK=KK-1.0
    IF (KKK.NE.0) XK=FLOAT(KKK)
    XITOP=AMINI(XII+XI2,XF+XJ)
    ITOP=10.*XITOP+1.
    XIBOT=AMAX1(ABS(XII-XI2),ABS(XF-XJ))
    IBOT=10.*XIBOT+1.
    DO 5 II=IBOT,ITOP,10
    XI=(II-1.)/10.
    JCOUNT=JCOUNT+1
    YMF(JCOUNT)=XMF
    YJ(JCOUNT)=XJ
    YF(JCOUNT)=XF
    YK(JCOUNT)=XK
    YI(JCOUNT)=XI
    JCMAX=JCOUNT
350 KVECT=DIAG $ COUNT=INIC
    LROW=LROW+1
    LCOL=LROW-1
    DO 6 JP=JJ,JTOP
    XJP=JP-1.0
    XFPTOP=XJP+XII+XI2
    FPTOP=10.*XFPTOP+1.
    XPBIG=AMAX1(XII,XI2,XJP)
    XFPBOT=AMAX1(ABS(XMF),2.0*XPBIG-XII-XI2-XJP)
    FPBOT=10.*XFPBOT+1.
    IF (XJP.EQ.XJ) FFBOT=F
    DO 7 FP=FPBOT,FPTOP,10
    XFP=(FP-1.)/10.
    KPTOP=2.*JP-1.
    IF (A.EQ.0.0) KPTOP=1
    IF (KKK.NE.0) KPTOP=1

```

```

KPBOT=1
IF (XJP.EQ.XJ.AND.XFP.EQ.XF) KPBOT=KK
DO 8 KP=KPBOT,KFTOP
XKP=KP-JP
IF (A.EQ.0.0) XKP=KP-1.0
IF (KKK.NE.0) XKP=FLOAT(KKK)
XIPTOP=AMIN1(XI1+XI2,XFP+XJP)
IPTOP=10.*XIPTOP+1.
XIPBOT=AMAX1(ABS(XI1-XI2),ABS(XFP-XJP))
IPBOT=10.*XIPBOT+1.
IF (XJP.EQ.XJ.AND.XFP.EQ.XF.AND.XKP.EQ.XK) IPBOT=II
DO 9 IP=IPBOT,IPTOP,10
XIP=(IP-1.)/10.
LCOL=LCOL+1
400 QUAD=0.0 $ STARK=0.0 $ ROT=0.0

```

C

```

IF (EQQ1.EQ.0.0) GO TO 500
IF (XF.NE.XFP) GO TO 500
IF (XJP-XJ.GT.2.0) GO TO 700
IF (XJP+XJ.LE.1.0) GO TO 500
IF (XK.NE.XKP) GO TO 600
IFA21=XIP+XJ-XF
P6=(-1)**IFA21
P7=SQRT((2.*XIP+1.)*(2.*XI+1.)*(2.*XJP+1.))
WL1=XJ $ WL2=2.0 $ WM=XJ $ WN=0.0 $ WL=XJP
CALL CLEBS
P3=1.0/W
IFA22=-XIP-XI-XJ-XJP
P4=(-1)**IFA22
QJ1=XIP $ QJ2=XI $ QJ3=2.0 $ QL1=XJ $ QL2=XJP $ QL3=XF
CALL SIXJ
P5=Q
P9=0.25*P6*P7*P3*P4*P5
IF (P9.EQ.0.0) GO TO 500
IFA23=XI2-XI1-XIP
V1=(-1)**IFA23
Z1=(2.*XF1+1.)*(2.*XI1+3.)*(XI1+1.)
Z2=XI1*(2.*XI1-1.)
V2=SQRT(Z1/Z2)
IFA24=-XI1-XI1-XI-XIP
V3=(-1)**IFA24
QJ1=XI1 $ QJ2=XI1 $ QL1=XI $ QL2=XIP $ QL3=XI2
CALL SIXJ
V4=Q
V=V1*V2*V3*V4
IF (EQQ2.EQ.0.0) GO TO 450
GO TO 460
450 U=0.0
GO TO 470
460 CONTINUE
IFA25=XI1-XI2-XI
U1=(-1)**IFA25
Z3=(2.*XI2+1.)*(2.*XI2+3.)*(XI2+1.)
Z4=XI2*(2.*XI2-1.)

```

```

U2=SQRT(Z3/Z4)
IFAZ6=-XI2-XI2-XI-XIP
U3=(-1)**IFAZ6
QJ1=XI2 $ QJ2=XI2 $ QL3=XI1
CALL SIXJ
U4=Q
U=U1*U2*U3*U4
470 CONTINUE
SPACEL=P9*(EQQ1*V+EQQ2*U)
ROT1=SQRT((2.*XJ+1.)/(2.*XJP+1.))
WM=-XK
CALL CLEPS
ROT2=W
WM=-XJ
CALL CLEBS
ROT3=W
490 QUAD=SPACEL*ROT1*ROT2*ROT3
C
500 IF (E(IDAT).EQ.0.0) GO TO 600
IF (ABS(XJ-XJP).GT.1.0) GO TO 700
IF (ABS(XF-XFP).GT.1.0) GO TO 700
IF (XK.NE.XKP) GO TO 600
IF (XI.NE.XIP) GO TO 700
IFAS1=2.*XFP-XMF+XJ+XI+XK+XJP
S1=(-1)**IFAS1
S2=SQRT((2.*XF+1.)*(2.*XFP+1.)*(2.*XJ+1.)*(2.*XJP+1.))
QJ1=XF $ QJ2=XFP $ QJ3=1.0 $ QL1=XJP $ QL2=XJ $ QL3=XI
CALL SIXJ
S3=Q
S4=0.0 $ S5=0.0
IF (XK.NE.XKP) GOTO 520
IFAS2=XJP-1.0-XK
S4=((-1)**IFAS2)/SQRT(2.*XJ+1.)
WL1=XJP $ WL2=1.0 $ WL=XJ $ WM=-XK $ WN=0.0
CALL CLEBS
S5=W
520 IFAS3=XFP-1.-XMF
S6=((-1)**IFAS3)/SQRT(2.*XF+1.)
WL1=XFP $ WL=XF $ WM=-XMF
CALL CLEBS
S7=W
SP=0. $ SM=0.
IF (XK.EQ.XKP) GOTO 590
WL1=XJ $ WL=JP $ WM=-XK $ WN=1.0
CALL CLEBS
SM=((-1)**(WL1-WL2+XKP))*W/SQRT(2.*WL+1.)
WN=-1.0
CALL CLEBS
SP=((-1)**(WL1-WL2+XKP))*W/SQRT(2.*WL+1.)
590 STARK=E(IDAT)*503.4036*S1*S2*S3*S6*S7*
1(S4*S5*AMU+(SP-SM)*BMU)
C
600 IF (XJP.NE.XJ) GO TO 700
IF (XFP.NE.XF) GO TO 700

```

```

IF (XIP.NE.XI) GO TO 700
DISTO=DJ*XJ*XJ*(XJ+1.)*(XJ+1.)+DK*XK*XK*XK*XK
1+DJK*XJ*(XJ+1.0)*XK*XK
IF (XK.EQ.XKP) ROT=BEFF*XJ*(XJ+1.)+(A-BEFF)*XK*XK-DISTO
IF (XKP.EQ.XK+2.0) ROT=((B-C)/4.0)*SQRT((XJ*(XJ+1.)-XK*(XK+1.))
1*(XJ*(XJ+1.)-(XK+1.)*(XK+2.))
IF (XKP.EQ.XK-2.) ROT=((B-C)/4.0)*SQRT((XJ*(XJ+1.)-XK*(XK-1.))
1*(XJ*(XJ+1.)-(XK-1.)*(XK-2.))

```

C

```

700 HAMIL(KVECT)=ROT+STARK+QUAD
KVMAX=KVECT
IF (HAMIL(KVECT).EQ.0.0) GO TO 720
IF (LSTSQ.GT.0) GOTO 720
IF (IFLAG1.GT.0) GO TO 720
WRITE(6,710)XMF,XJ,XF,XK,XI,XJP,XFP,XKP,XIP,KVECT,HAMIL(KVECT)
710 FORMAT(4X,5(F4.1,3X),6X,4(F4.1,3X),7X,I4,7X,E15.8)
GO TO 730
720 IF (KVECT.NE.DIAG) GO TO 730
MCCOUNT=MCCOUNT+1
IF (IFLAG5.GT.0) GOTO 730
IF (LSTSQ.GT.0) GOTO 730
WRITE(6,725)XMF,XJ,XF,XK,XI,LROW,LCOL,HAMIL(KVECT),MCCOUNT
725 FORMAT(4X,5(F4.1,3X),6X,I2,7X,I2,7X,E15.8,9X,I4)

```

C

```

730 KVECT=KVECT+COUNT
COUNT=COUNT+1
9 CONTINUE
8 CONTINUE
7 CONTINUE
6 CONTINUE
740 DIAG=DIAG+IN
IN=IN+1
INIC=INIC+1
5 CONTINUE
4 CONTINUE
3 CONTINUE
2 CONTINUE

```

C

```

IDIMEN=LROW
CALL EIGEN(HAMIL,DEIGEN,IDIMEN,IFLAG2)
IF (IFLAG4.GT.0) GO TO 810
IF (LSTSQ.GT.0) GOTO 810
WRITE(6,800)
800 FORMAT(2X,///,4X,*EIGENVALUE*,4X,*STATE NO*,//)
810 CONTINUE
DO 825 III=1,IDIMEN
ICOUNT=(I*III+III)/2
JCONT=JCONT+1
EIG(JCONT)=HAMIL(ICOUNT)
IF (IFLAG4.GT.0) GO TO 825
IF (LSTSQ.GT.0) GOTO 825
WRITE(6,820) HAMIL(ICOUNT),JCONT
820 FORMAT(2X,E15.8,3X,I4)
825 CONTINUE

```

```

IF (IFLAG2.GT.0) GO TO 857
IF (LSTSQ.GT.0) GOTO 857
WRITE(6,830)
830 FORMAT(2X,/,6X,*COEF*,9X,*ID NO*,6X,*STATE NO*,/)
ILIMIT=IDIMEN*IDIMEN
LL=LL+IDIMEN
DO 855 ILABEL=1,ILIMIT
LABEL=LABEL+1
IF (LABEL.EQ.LL) LABEL=LSTART
IF (LABEL.EQ.LSTART) LCOUNT=LCOUNT+1
IF (IFLAG3.GT.0.AND.DEIGEN(ILABEL)**2.LT.0.2) GO TO 845
DSQR=DEIGEN(ILABEL)*DEIGEN(ILABEL)
WRITE(6,840) DEIGEN(ILABEL),LABEL,LCOUNT
840 FORMAT(2X,E15.8,5X,I4,9X,I4)
845 CONTINUE
IF (MOD(ILABEL, IDIMEN).EQ.0) WRITE (6,850)
850 FORMAT(2X,/)
855 CONTINUE
LSTART=LABEL+1
857 CONTINUE
1 CONTINUE
WRITE(6,860)
860 FORMAT(2X,////////////////////,7X,*FREQ*,9X,*STATE 1*,4X,*STATE 2*,/)
IFREQ=1
DO 875 JCNT=1,JCMAX
IF (YJ(JCNT).LT.JJJ.OR.YJ(JCNT).GT.JJJ+IDELJ) GO TO 875
JCNT1=JCNT+1
DO 873 KCNT=JCNT1,JCMAX
IF (YJ(KCNT).LT.JJJ.OR.YJ(KCNT).GT.JJJ+IDELJ) GO TO 873
IF (ABS(YMF(KCNT)-YMF(JCNT)).GT.IDELMF) GO TO 873
IF (ABS(YJ(KCNT)-YJ(JCNT)).GT.IDELJ) GO TO 873
IF (ABS(YF(KCNT)-YF(JCNT)).GT.IDELF) GO TO 873
IF (ABS(YK(KCNT)-YK(JCNT)).GT.IDELK) GO TO 873
IF (ABS(YI(KCNT)-YI(JCNT)).GT.IDELI) GO TO 873
HAMIL(IFREQ)=ABS(EIG(JCNT)-EIG(KCNT))
IF (HAMIL(IFREQ).GT.FRMAX) GO TO 873
IF (HAMIL(IFREQ).LT.FRMIN) GO TO 873
HAMIL(IFREQ+1666)=JCNT
HAMIL(IFREQ+3332)=KCNT
IFREQ=IFREQ+1
IF (IFREQ.EQ.1650) WRITE(6,870)
870 FORMAT(/,2X,*CAREFUL----YOU'VE GOT A SHITLOAD OF TRANSITIONS*,/)
873 CONTINUE
875 CONTINUE
IFM2=IFREQ-2
DO 879 II=1,IFM2
IIP1=II+1
IFM1=IFREQ-1
DO 877 IJ=IIP1,IFM1
IF (HAMIL(II).GE.HAMIL(IJ)) GO TO 877
TEMP=HAMIL(II)
HAMIL(II)=HAMIL(IJ)
HAMIL(IJ)=TEMP
TEMP=HAMIL(II+1666)

```

```

HAMIL(I1+1666)=HAMIL(IJ+1666)
HAMIL(IJ+1666)=TEMP
TEMP=HAMIL(I1+3332)
HAMIL(I1+3332)=HAMIL(IJ+3332)
HAMIL(IJ+3332)=TEMP
877 CONTINUE
879 CONTINUE
DO 885 JFREQ=1,IFM1
LJCNT=HAMIL(JFREQ+1666)
LKCNT=HAMIL(JFREQ+3332)
LCALC(JFREQ, IDAT)=65536*LJCNT+LKCNT
WRITE(6,880) HAMIL(JFREQ),LJCNT,LKCNT
880 FORMAT(2X,E15.8,5X,I4,9X,I4)
885 CONTINUE
IF (NFIT.EQ.0) GOTO 85
CALL FITPAR
GOTO (900,999) ILL
900 CONTINUE
IF (I5.LT.NTOT) GOTO 90
999 STOP
END

```

C

```

SUBROUTINE CLEBS
COMMON/CLBCOM/WL1,WL2,WL,WM,WN,W
COMMON FACT(20)
IF (WM.GT.WL1)GOTO 1
IF (WN.GT.WL2)GOTO 1
IF (WL.GT.(WL1+WL2))GOTO1
IF(WM.LT.(-WL1))GOTO1
IF (WN.LT.(-WL2))GOTO1
IF (WL.LT.ABS(WL1-WL2))GOTO1
IF ((WM+WN).GT.WL)GOTO1
IF ((WM+WN).LT.(-WL))GOTO1
GOTO9
1 W=0.0
GOTO 10
9 AA=FACT(WL+WL1-WL2+1.5)
AB=FACT(-L-WL1+WL2+1.5)
AC=FACT(WL1+WL2-WL+1.5)
AD=FACT(WL+WM+WN+1.5)
AE=FACT(WL-WM-WN+1.5)
AG=FACT(WL+WL1+WL2+2.1)
AH=FACT(WL1-WM+1.1)
AI=FACT(WL2-WN+1.1)
AJ=FACT(WL1+WM+1.1)
AK=FACT(WL2+WN+1.1)
AZ=SQRT(AA*AB*AC*AD*AE*1.0)/SQRT(AG*AH*AI*AJ*AK*1.0)
-API=AMAX1(0.0,WL2-WL1+WM+WN)+1.0
IAP2=AMIN1(WL+WM+WN,WL-WL1+WL2)+1.0
AY=0.0
DO 2 IP=IAP1,IAP2
P=IP-1.0
IPHASE=P+WL2+WN
AQ=(-1.0)**IPHASE

```

```

AR=SQRT(2.0*WL+1.0)
AS1=FACT(WL+WL2+WL3+WM-P+1.1)
AS2=FACT(WL1-WM+P+1.1)
AT1=FACT(WL-WL1+WL2-P+1.1)
AT2=FACT(WL+WM+WN-P+1.1)
AT3=FACT(P+1.1)
AT4=FACT(P+WL1-WL2-WM-WN+1.1)
AY=AY+(AQ*AR*AS1*AS2)/(AT1*AT2*AT3*AT4)
2 CONTINUE
W=A2*AY
10 CONTINUE
RETURN
END

```

C

```

SUBROUTINE SIXJ
COMMON/SXJCOM/QJ1,QJ2,QJ3,QL1,QL2,QL3,Q
COMMON/DLTCOM/QY1,QY2,QY3,DLT
COMMON FACT(20)
DIMENSION QD(4)
IF (QJ3.GT.(QJ1+QJ2)) GO TO 1
IF (QJ3.LT.ABS(QJ1-QJ2)) GO TO 1
IF (QJ3.GT.(QL1+QL2)) GO TO 1
IF (QJ3.LT.ABS(QL1-QL2)) GO TO 1
IF (QL3.GT.(QJ1+QL2)) GO TO 1
IF (QL3.LT.ABS(QJ1-QL2)) GO TO 1
IF (QL3.GT.(QJ2+QL1)) GO TO 1
IF (QL3.LT.ABS(QJ2-QL1)) GO TO 1
GO TO 2
1 Q=0.0
RETURN
2 QY1=QJ1 $QY2=QJ2 $QY3=QJ3
CALL DELTA
QD(1)=DLT
QY1=QJ1 $QY2=QL2 $QY3=QL3
CALL DELTA
QD(2)=DLT
QY1=QL1 $QY2=QJ2 $QY3=QL3
CALL DELTA
QD(3)=DLT
QY1=QL1 $QY2=QL2 $QY3=QJ3
CALL DELTA
QD(4)=DLT
QD2=SQRT(QD(1)*QD(2)*QD(3)*QD(4))
IQMN=AMAX1(QJ1+QJ2+QJ3,QJ1+QL2+QL3,QL2+QL1+QJ3,QL1+QJ2+QL3)+1.0
IQNM=AMIN1(QJ1+QJ2-QJ3,QJ2+QJ3-QJ1,QJ3+QJ1-QJ2,QJ1+QL2-QL3,
1QL2+QL3-QJ1,QL3+QJ1-QL2,QL1+QJ2-QL3,QJ2+QL3-QL1,
2QL3+QL1-QJ2,QL1+QL2-QJ3,QL2+QJ3-QL1,QJ3+QL1-QL2)
QK2=0.0
ILOOP=IQMN+IQNM
DO 3 IT=IQMN,ILOOP
T=IT-1
IFASE=T
QAL=FACT(T+2.1)*((-1)**IFASE)
QB1=FACT(T-QJ1-QJ2-QJ3+1.1)

```



```

QB2=FACT(T-QJ1-QL2-QL3+1.1)
QB3=FACT(T-QL1-QJ2-QL3+1.1)
QB4=FACT(T-QL1-QL2-QJ3+1.1)
QB5=FACT(QJ1+QJ2+QL1+QL2-T+1.1)
QB6=FACT(QJ3+QJ2+QL2+QL3+1.1-T)
QB7=FACT(QJ1+QJ3+QL1+QL3+1.1-T)
QK2=QK2+QA1/(QB1*QB2*QB3*QB4*QB5*QB6*QB7)
3 CONTINUE
Q=QD2*QK2
RETURN
END

```

C

```

SUBROUTINE DELTA
COMMON/DLTCOM/QY1,QY2,QY3,DLT
COMMON FACT(20)
DF1=FACT(QY1+QY2-QY3+1.1)
DF2=FACT(QY2+QY3-QY1+1.1)
DF3=FACT(QY3+QY1-QY2+1.1)
DF4=FACT(QY1+QY2+QY3+2.1)
DLT=DF1*DF2*DF3/DF4
RETURN
END

```

C

```

SUBROUTINE EIGEN(HAMIL,DEIGEN,N,MV)
DIMENSION HAMIL(5000),DEIGEN(10000)
5 RANGE=1.0E-12
IF(MV-1) 10,25,10
10 IQ=-N
DO 20 J=1,N
IQ=IQ+N
DO 20 I=1,N
IJ=IQ+I
DEIGEN(IJ)=0.0
IF (I-J) 20,15,20
15 DEIGEN(IJ)=1.0
20 CONTINUE
25 ANORM=0.0
DO 35 I=1,N
DO 35 J=I,N
IF (I-J) 30,35,30
30 IA=I+(J*J-J)/2
ANORM=ANORM+HAMIL(IA)*HAMIL(IA)
35 CONTINUE
IF (ANORM) 165,165,40
40 ANORM=1.414*SQRT(ANORM)
ANRMX=ANORM*RANGE/FLOAT(N)
IND=0
THR=ANORM
45 THR=THR/FLOAT(N)
50 L=1
55 M=L+1
60 MQ=(M*M-M)/2
LQ=(L*L-L)/2
LM=L+MQ

```

```

62 IF (ABS(HAMIL(LM))-THR) 130,65,65
65 IND=1
   LL=L+LQ
   MM=M+MQ
   X=0.5*(HAMIL(LL)-HAMIL(MM))
68 Y=-HAMIL(LM)/SQRT(HAMIL(LM)*HAMIL(LM)+X*X)
   IF (X) 70,75,75
70 Y=-Y
75 SINX=Y/SQRT(2.0*(1.0+SQRT(1.0-Y*Y)))
   SINX2=SINX*SINX
78 COSX=SQRT(1.0-SINX2)
   COSX2=COSX*COSX
   SINCX=SINX*COSX
   ILQ=N*(L-1)
   IMQ=N*(M-1)
   DO 125 I=1,N
     IQ=(I*I-I)/2
     IF (I-L) 80,115,80
80 IF (I-M) 85,115,90
85 IM=I+MQ
   GO TO 95
90 IM=M+IQ
95 IF(I-L) 100,105,105
100 IL=I+LQ
   GO TO 110
105 IL=L+IQ
110 X=HAMIL(IL)*COSX-HAMIL(IM)*SINX
   HAMIL(IM)=HAMIL(IL)*SINX+HAMIL(IM)*COSX
   HAMIL(IL)=X
115 IF (M-1) 120,125,120
120 IIR=ILQ+I
   IMR=IMQ+I
   X=DEIGEN(IIR)*COSX-DEIGEN(IMR)*SINX
   DEIGEN(IMR)=DEIGEN(IIR)*SINX+DEIGEN(IMR)*COSX
   DEIGEN(IIR)=X
125 CONTINUE
   X=2.*C*HAMIL(LM)*SINCX
   Y=HAMIL(LL)*COSX2+HAMIL(MM)*SINX2-X
   X=HAMIL(LL)*SINX2+HAMIL(MM)*COSX2+X
   HAMIL(LM)=(HAMIL(LL)-HAMIL(MM))*SINCX+HAMIL(LM)*(COSX2-SINX2)
   HAMIL(LL)=Y
   HAMIL(MM)=X
130 IF (M=N) 135,140,135
135 M=M+1
   GO TO 60
140 IF (L=(N-1)) 145,150,145
145 L=L+1
   GO TO 55
150 IF (IND=1) 160,155,160
155 IND=0
   GO TO 50
160 IF (THR-ANRMX) 185,185,45
165 CONTINUE
185 CONTINUE

```

```

RETURN
END
SUBROUTINE FITPAR
COMMON/FITCOM/FREQ(200,5),FCALC(200,5),DERIV(200,5,7),
LAO(7),DELA(7),D(7,8),LCALC(200,5),NORD(7),IDEN(200,5),
2NP(5),E(5),A,B,C,EQ1,EQ2,AMU,BMU,CONST,DELFQ,
3I5,ICYC,IDAT,IFLAG6,ILL,IFM1,INCR,JLST,LSTSQ,
4MPAR,NPAR,NFIT,NTOT,STDV,STDVP
COMMON/BIGCOM/HAMIL(5000),DEIGEN(10000),EIG(1000)
DIMENSION PAR(7),NAME(8),FCDER(200,5,8),SD(7),L(8),CORR(7)
EQUIVALENCE (FCALC(1),FCDER(1)),(A,PAR(1))
EQUIVALENCE (NORD(1),L1),(NORD(2),L2),(NORD(3),L3),(NORD(4),L4),
1(NORD(5),L5),(NORD(6),L6),(NORD(7),L7)
DATA NAME/#AROT#,#BROT#,#CROT#,#EQQ1#,#EQQ2#,#ADMU#,
1#BDMU#,# #/
C
IF (IDAT.NE.NFIT) GOTO 10
GOTO(10,2),ICYC
C
STEPS IN DERIV CALC LCOP
2 ICYC=1
PAR(JLST)=CONST
10 K=1
NP=NPT(IDAT)
DO 14 J=1,NP
K1=IDEN(J,IDAT)
N=1
9 DO 13 I=1,IFM1
IF(LCALC(1,IDAT)-K1) 13,12,13
12 FCDER(J,IDAT,1+LSTSQ)=HAMIL(I)
GOTO 14
13 CONTINUE
GOTO(17,18),N
17 N=2
I1=K1/65536
I2=K1-65536*I1
K1=65536*I2+I1
GOTO 9
18 WRITE(6,1013)I1,I2
K=2
14 CONTINUE
GOTO(16,43),K
16 IF(LSTSQ) 100,20,100
20 IF(STDVP) 60,22,60
22 DO 24 J=1,NP
24 HAMIL(J)=FCALC(J,IDAT)
IF (IDAT.EQ.NFIT) GOTO 52
RETURN
43 WRITE(6,1043)(HAMIL(I),I=1,IFM1)
I5=NTOT
RETURN
52 IF(STDVP)60,54,60
54 MPAR=NPAR+1
60 IF (IDAT.NE.NFIT) GOTO 22
STDV=0.0 $ NP(1)=0.0

```

```

DO 62 I=1,NFIT
NP=NPT(I)
DO 61 J=1,NP
61 STDV=STDV+((FREQ(J,I)-FCALC(J,I))**2)
NTPT=NTPT+NPT(I)
62 CONTINUE
CONST=NTPT-NPAR
IF(CONST) 64,63,64
63 CONST=1.0
64 STDV=SQRT(STDV/CONST)
IF(STDVP) 70,76,70
70 WRITE(6,1070) STDV,NTPT,NPAR
WRITE(6,1071)
DO 72 I=1,NPAR
STDVA=STDV*SQRT(D(I,I))
JP=NORD(I)
CONST=PAR(JP)-AO(I)
72 WRITE(6,1072) NAME(JP),PAR(JP),STDVA,CONST
IF(STDV/STDVP<0.9) 80,74,74
74 WRITE(6,1073)I5
WRITE(6,1074)
DO 77 K=1,NFIT
NF=NPT(K)
WRITE(6,1077) K
1077 FORMAT(//,*DATA SET*,I5)
DO 75 J=1,NP
SIGMA=0.0
DO 73 I1=1,NEAR
CONST=0.0
DO 71 I2=1,NEAR
71 CONST=CONST+D(I1,I2)*DERIV(J,K,I2)
73 SIGMA=SIGMA+DERIV(J,K,I1)*CONST
SIGMA=SQRT(SIGMA)*STDV
CONST=FREQ(J,K)-FCALC(J,K)
75 WRITE(6,1075) FREQ(J,K),FCALC(J,K),CONST,SIGMA
77 CONTINUE
I5=NTOT
RETURN
76 WRITE(6,1076) STDV
80 STDVP=STDV
100 IF (IDAT.NE.NFIT) GOTO 22
LSTSQ=LSTSQ+1
IF(LSTSQ-NPAR) 102,102,130
102 JLST=NORD(LSTSQ)
CONST=PAR(JLST)
PAR(JLST)=CONST+DELA(LSTSQ)
IF(LSTSQ-1) 105,120,105
105 I5=I5-1
120 ICYC=2
RETURN
130 LSTSQ=0
DO 132 I=1,7
DO 132 J=1,8
132 D(I,J)=0.0

```

```

      GO TO (135,133),INCR
133 DO 134 I=1,NPAR
      DO 134 K=1,NFIT
      NP=NPT(K)
      DO 134 J=1,NP
134 DERIV(J,K,I)=(DERIV(J,K,I)-FCALC(J,K))/DELA(I)
      GO TO 142
135 INCR=2
      DO 138 I=1,NPAR
      SUM=0.0
      CONST=0.0
      DENOM=1.0/DELA(I)
      DO 136 K=1,NFIT
      NP=NPT(K)
      DO 136 J=1,NP
      DNUM=DERIV(J,K,I)-FCALC(J,K)
      IF(DNUM.EQ.0.0) GO TO 136
      CONST=CONST+DELFQ
      SUM=SUM+ABS(DNUM)
136 DERIV(J,K,I)=DNUM*DENOM
      IF(CONST) 137,137,138
137 K=NORD(I)
      WRITE(6,1137) NAME(K)
C     SET DISASTER TEST VARIABLE AND QUIT
      ILL=2
      RETURN
138 DELA(I)=DELA(I)*CONST/SUM
      WRITE(6,1138)(DELA(I),I=1,NPAR)
      WRITE(6,1139) DELFQ
142 CONTINUE
      IF (IFLAG6.GT.0) GOTO 145
      WRITE(6,1142) NAME(L1),NAME(L2),NAME(L3),NAME(L4),
      LNAME(L5),NAME(L6),NAME(L7)
      DO 143 K=1,NFIT
      NP=NPT(K)
      DO 143 J=1,NP
143 WRITE(6,1143) (DERIV(J,K,I),I=1,NPAR)
145 CONST=0.0
      DO 150 K2=1,NFIT
      NP=NPT(K2)
      DO 150 J=1,NP
      CONST=1.0
      STOG=FREQ(J,K2)-FCALC(J,K2)
      DO 150 I=1,NPAR
      DO 140 K=1,I
140 D(I,K)=DERIV(J,K2,I)*DERIV(J,K2,K)+D(I,K)
150 D(I,MPAR)=STOG*DERIV(J,K2,I)+D(I,MPAR)
      DO 154 I=1,NPAR
      DO 152 K=1,I
152 D(I,K)=D(I,K)*CONST
154 D(I,MPAR)=D(I,MPAR)*CONST
C     INVERT D AND SOLVE FOR PAR ADJUSTMENTS
      DETDP=1.0

```

```

L(MPAR)=MPAR
DO 220 I=1, NPAR
SD(I)=1.0/SQRT(D(I,I))
C SCALE RIGHT-HAND SIDE (ERROR VECTOR)
D(I,MPAR)=D(I,MPAR)*SD(I)
C START SUBSCRIPT ARRAY IN ORDER
L(I)=I
DO 220 J=1, I
C SCALE D AND FILL EMPTY TRIANGLE
D(I,J)=D(I,J)*SD(I)*SD(J)
220 D(J,I)=D(I,J)
C ENTER INVERSION LOOP
I=1
225 DO 250 J=1, NPAR
IF(I-J) 230, 250, 230
230 CONST=D(L(J),L(I))
D(L(J),L(I))=0.0
DO 240 K=1, MPAR
240 D(L(J),L(K))=D(L(J),L(K))-D(L(I),L(K))*CONST
250 CONTINUE
I=I+1
IF(I-NPAR)252, 260, 270
252 CONST=D(L(I),L(I))
K=I
IPI=I+1
DO 256 J=IPI, NPAR
IF(CONST-D(L(J),L(J)))254, 254, 256
254 CONST=D(L(J),L(J))
K=J
256 CONTINUE
II=L(I)
L(I)=L(K)
L(K)=II
GO TO 262
260 CONST=D(L(I),L(I))
262 IF(CONST-1.0E-8)300, 264, 264
264 D(L(I),L(I))=1.0
DO 266 J=1, MPAR
266 D(L(I),L(J))=D(L(I),L(J))/CONST
DETFP=DETFP*CONST
GO TO 225
270 I=NPAR
C I=NPAR IF THE WHOLE ARRAY WAS INVERTED
272 DO 280 J=1, I
AO(L(J))=PAR(NORD(L(J)))
PAR(NORD(L(J)))=AO(L(J))+D(L(J),MPAR)*SD(L(J))
DO 280 K=1, I
280 D(L(J),L(K))=D(L(J),L(K))*SD(L(J))*SD(L(K))
WRITE(6, 1280)DETFP, NAME(L1), NAME(L2), NAME(L3),
1NAME(L4), NAME(L5), NAME(L6), NAME(L7)
DO 290 I=1, NPAR
IF(D(I,I))282, 282, 284
282 SD(I)=1.0
GO TO 286

```

```

284 SD(I)=1.0/SQRT(D(I,I))
286 DO 288 J=1,I
288 CORR(J)=D(I,J)*SD(I)*SD(J)
290 WRITE(6,1290) (CORR(J),J=1,I)
      I5=I5-1
      RETURN
C      D IS SINGULAR IF LINE 300 IS REACHED; THROW OUT THE EXTRA
C      PARAMETER ADJUSTMENTS
300 DO 310 J=I,NPAR
      DO 308 K=1,NPAR
        D(L(J),L(K))=0.0
308 D(L(K),L(J))=0.0
310 AO(L(J))=PAR(NORD(L(J)))
      I=I-1
      WRITE(6,1310) I,(L(J),J=1,NPAR)
      GO TO 272
1013 FORMAT(27HUNABLE TO MATCH INPUT LINE,2I6)
1042 FFORMAT(17HIDENTITY CRISIS,,I4,16F CALC LINES, BUT,I4,16H
1 OBSERVED LINES.)
1043 FORMAT(*OFREQUENCIES AND WEIGHTS*//((1PE20.7,E20.5))
1056 FORMAT(36HOPREQ ERROR OUT OF TOLERANCE IN LINE,I4)
1070 FORMAT(*OST. DEV. =*,1PE10.3,* FOR*,I4,* POINTS AND*,I2,
1* ADJUSTED PARAMETERS*)
1071 FORMAT(*ONAME*,9X,*PARAMETER*,8X,*ST. DEV. ADJUSTMENT*/)
1072 FORMAT(1X,A4,1PE20.7,2E15.4)
1073 FORMAT(25HOCALCULATION COMPLETED IN,I3,8H CYCLES./)
1074 FORMAT(*O*,/,*O*,10X,*FREQ(OBS)*,14X,*FREQ(CALC)*,9X,*DIFF. (OBS-
1CALC)*,9X,*SIGMA*/)
1075 FORMAT(1P2E23.9,2E20.4)
1076 FORMAT(*OST. DEV. OF INITIAL GUESS =*,1PE10.3/)
1137 FORMAT(* ALL DERIVS OF *,A4,* VANISH*)
1138 FORMAT(*ODELAS ARE*,1P7E14.3)
1139 FORMAT(* FOR AVERAGE ABSOLUTE FREQUENCY INCREMENTS OF *,1PE10.3)
1142 FORMAT(*ODERIV MATRIX WITH COLUMN LABELS*/7(10X,A4,4X)/)
1143 FORMAT(1P7E18.7)
1280 FORMAT(*O*/*SCALED NORMAL EQUATIONS DETERMINANT =*,1PE10.3/*OCORR
RELATION MATRIX FOR FOLLOWING FIT DATA, INCLUDING PARAMETER LABELS
2/7(7X,A4,2X))
1290 FORMAT(7F13.6)
1310 FORMAT(* ONLY*,I3,* INDEPENDENT PARAMETERS, LS ARE*,7I5)
      END
<BOTTOM OF FILE>

```

References for Appendix II

1. G. R. Tomasevich, Ph.D. Thesis, Harvard University, 1970.
2. C. H. Townes and A. L. Schawlow, Microwave Spectroscopy (McGraw-Hill), New York, 1955).
3. W. H. Flygare and W. D. Gwinn, J. Chem. Phys. **36**, 787 (1962).
4. J. E. Wollrab, Rotational Spectra and Molecular Structure (Academic Press, New York, 1967).
5. S. J. Harris, Ph.D. Thesis, Harvard University, 1975.

This report was done with support from the Department of Energy. Any conclusions or opinions expressed in this report represent solely those of the author(s) and not necessarily those of The Regents of the University of California, the Lawrence Berkeley Laboratory or the Department of Energy.

Reference to a company or product name does not imply approval or recommendation of the product by the University of California or the U.S. Department of Energy to the exclusion of others that may be suitable.